Department of Biotechnology and Chemical Technology

Vapor–Liquid Equilibrium and Excess Enthalpies: Measurements and Modeling for Process Industry

Helena Laavi

A!
DOCTORAL DISSERTATIONS

Aalto University publication series
DOCTORAL DISSERTATIONS 121/2013

Vapor–Liquid Equilibrium and Excess Enthalpies: Measurements and Modeling for Process Industry

Helena Laavi

A doctoral dissertation completed for the degree of Doctor of Science (Technology) to be defended, with the permission of the Aalto University School of Chemical Technology, at a public examination held at the Auditorium KE2 (Komppa Auditorium) of the school on 11 October 2013 at 12.

Aalto University
School of Chemical Technology
Department of Biotechnology and Chemical Technology
Research Group of Chemical Engineering

Supervising professor
Professor Ville Alopaeus

Thesis advisors
Dr. Juha-Pekka Pokki
Dr. Petri Uusi-Kyyny

Preliminary examiners
Dr./CNRS res. prof. Vladimir Mayer, Blaise Pascal University Institute of Chemistry of Clermont-Ferrand, France

Dr./Ass.prof. Kaj Thomsen, Technical University of Denmark, Denmark

Opponent
Professor Georgios Kontogeorgis, Technical University of Denmark, Denmark

Aalto University publication series
DOCTORAL DISSERTATIONS 121/2013

ISBN 978-952-60-5271-7 (printed)
ISBN 978-952-60-5272-4 (pdf)
ISSN-L 1799-4934
ISSN 1799-4934 (printed)
ISSN 1799-4942 (pdf)
http://urn.fi/URN:ISBN:978-952-60-5272-4

Unigrafia Oy
Helsinki 2013

Finland

441 697
Printed matter

Aalto University

Abstract

Aalto University, P.O. Box 11000, FI-00076 Aalto www.aalto.fi

Author
Helena Laavi

Name of the doctoral dissertation
Vapor–Liquid Equilibrium and Excess Enthalpies: Measurements and Modeling for Process Industry

Publisher School of Chemical Technology

Unit Department of Biotechnology and Chemical Technology

Series Aalto University publication series DOCTORAL DISSERTATIONS 121/2013

Field of research Chemical Engineering

Manuscript submitted 16 April 2013 **Date of the defence** 11 October 2013

Permission to publish granted (date) 18 June 2013 **Language** English

☐ **Monograph** ☒ **Article dissertation (summary + original articles)**

Abstract

The purpose of this work was to examine vapor–liquid equilibria (VLE) together with excess enthalpies (H^E) in order to formulate thermodynamic models for the studied systems to meet the needs of process industry.

A static total pressure apparatus, a circulation still, and a headspace gas-chromatograph were used to obtain VLE data. A SETARAM C80 calorimeter with a flow mixing cell was implemented and used for H^E measurements and an Anton Paar DMA 512P vibrating tube densimeter for excess volumes (V^E). The parallel use of different VLE apparatuses widened the scope of the experiments and ensured the high quality of the VLE data.

The studied binary systems consisted of a group of alcohols with alkanes, ethers, esters, and a ketone. Additionally, binary mixtures of ethers and nitriles were studied. The components were selected based on their relevance to chemical industry and to their potential for supporting the sustainable development of eco-friendlier chemical processes.

The measured VLE data were modeled by using the Hayden–O'Connell method with the chemical theory for the vapor phase fugacities and the Wilson model, NRTL, UNIQUAC, or UNIFAC model for the liquid phase activity coefficients. The inclusion of also H^E data improved the model applicability beyond the original temperature and pressure ranges.

The parallel thermodynamic measurements produced data of good quality. The consistency of the data was checked by applying the area test, the point test, and the infinite dilution test on the measured data. For the static total pressure apparatus, the method of Barker was used to reduct the pTz data to $pTxy$ data.

Keywords vapor–liquid equilibrium, excess enthalpy, excess volume, flow calorimeter, circulation still, headspace, static total pressure apparatus

ISBN (printed) 978-952-60-5271-7 **ISBN (pdf)** 978-952-60-5272-4

ISSN-L 1799-4934 **ISSN (printed)** 1799-4934 **ISSN (pdf)** 1799-4942

Location of publisher Helsinki **Location of printing** Helsinki **Year** 2013

Pages 120 **urn** http://urn.fi/URN:ISBN:978-952-60-5272-4

A! Aalto-yliopisto

Tiivistelmä

Aalto-yliopisto, PL 11000, 00076 Aalto www.aalto.fi

Tekijä
Helena Laavi

Väitöskirjan nimi
Höyry-nestetasapaino ja eksessientalpia: Mittauksia ja malleja prosessiteollisuuden tarpeisiin

Julkaisija Kemian tekniikan korkeakoulu

Yksikkö Biotekniikan ja kemian tekniikan laitos

Sarja Aalto University publication series DOCTORAL DISSERTATIONS 121/2013

Tutkimusala Kemian laitetekniikka

Käsikirjoituksen pvm 16.04.2013 **Väitöspäivä** 11.10.2013

Julkaisuluvan myöntämispäivä 18.06.2013 **Kieli** Englanti

☐ **Monografia** ☒ **Yhdistelmäväitöskirja (yhteenveto-osa + erillisartikkelit)**

Tiivistelmä

Tässä työssä mitattiin höyry-nestetasapainoja (VLE) ja eksessientalpioita (H^E), joiden pohjalta laadittiin termodynaamisia malleja tutkituille kaksi-komponenttisysteemeille. Tutkitut systeemit ja näiden mallit ovat hyödyksi prosessiteollisuudelle.

Höyry-nestetasapainojen mittaamiseen käytettiin staattista kokonaispainemittalaitteistoa, lasista kierrätysmittalaitteistoa ja headspace- mittalaitetta yhdistettynä kaasukromatografiin. Eksessientalpiat mitattiin sekoituskennolla varustetulla SETARAM C80 –virtauskalorimetrillä, joka otettiin käyttöön tässä työssä. Anton Paarin DMA 512P –mallista tiheysmittaria käytettiin eksessitilavuuksien (V^E) määrittämiseen. Eri VLE-mittausmenetelmien rinnakkainen käyttö mahdollisti laajemman mittausalueen ja paransi mittausten laatua.

Tutkitut kaksi-komponenttisysteemit voitiin jakaa viiteen ryhmään. Systeemit muodostivat neljä ryhmää, joissa alkoholi oli toisena komponenttina ja toisena komponenttina oli joko alkaani, eetteri, esteri tai ketoni. Lisäksi viidenteen ryhmään kuuluivat komponenttiparit, joista toinen oli eetteri ja toinen nitriili. Komponenttien valinnoissa huomioitiin niiden merkitys prosessiteollisuudessa sekä ympäristöystävällisempien prosessien kehityksessä. Höyry-nestetasapainojen mittaustulokset mallinnettiin käyttämällä Hayden-O'Connell –menetelmää höyryfaasin fugasiteettien ja Wilson, NRTL, UNIQUAC tai UNIFAC-mallia nestefaasin aktiivisuuskertoimien määrittämiseen. Eksessientalpiat otettiin mukaan termodynaamiseen malliin, jota voitiin tämän ansiosta käyttää laajemmalla lämpötila- ja painealueella. Rinnakkaiset mittaukset tuottivat laadukasta tietoa aineominaisuuksista. Mittausten laatu tarkistettiin käyttämällä kolmea konsistessitestiä, joita kutsutaan pinta-alatestiksi, pistetestiksi ja äärettömän laimennoksen testiksi. Staattisella kokonaispainelaitteella saadut pTz-mittaustulokset redusoitiin $pTxy$-mittaustuloksiksi.

Avainsanat höyry-nestetasapaino, eksessientalpia, eksessitilavuus, virtauskalorimetri

ISBN (painettu) 978-952-60-5271-7 **ISBN (pdf)** 978-952-60-5272-4

ISSN-L 1799-4934 **ISSN (painettu)** 1799-4934 **ISSN (pdf)** 1799-4942

Julkaisupaikka Helsinki **Painopaikka** Helsinki **Vuosi** 2013

Sivumäärä 120 **urn** http://urn.fi/URN:ISBN:978-952-60-5272-4

Preface

The research work presented in this thesis was was completed during the years 2006-2013 in the Chemical Engineering research group at the Aalto University School of Chemical Technology (known as Helsinki University of Technology until the end of the year 2009). The financial support from Neste Oil Oyj, the Graduate School in Chemical Engineering (GSCE), the Research Foundation of Helsinki University of Technology, Academy of Finland, and Jenny and Antti Wihuri Foundation are gratefully acknowledged.

I want to express my gratitude to my supervisors professor Juhani Aittamaa who offered me the opportunity to begin my postgraduate studies, and professor Ville Alopaeus who eventually succeeded in carrying through my half-finished work. Without their support this work would have ended unfinished.

All my co-authors deserve special thanks for their valuable contributions to this work. In particular, I want to thank Dr. Juha-Pekka Pokki who has patiently and wisely answered hundreds of questions along with his own work. Also Dr. Petri Uusi-Kyyny provided equally important support when I tried to find solutions to many encountered research problems and is warmly thanked for that. Their endless enthusiasm about chemical thermodynamics combined with their deep understanding of both theory and practice have been indispensable.

I also want to thank Sirpa Aaltonen and Lasse Westerlund for their kindness and for handling all the administrative duties in the laboratory. The KeLaTeSu personnel as a whole formed an inspiring, creative, and friendly working environment. Especially, the open-minded conversations in the coffee room have been like a refreshing oasis when my mind was saturated with my research problems.

My warmest thanks go to my parents Anneli and Pertti, and to my dear

twin sister Elina who always encouraged and supported me whenever needed.

I'm also indebted to you all, my dear friends, who supported me during my post-graduate studies. An everlasting quote describes the course of this eventful project:

See, I am doing a new thing!
Now it springs up; do you not perceive it?
I am making a way in the wilderness
and streams in the wasteland.
Isaiah 43:19

Helsinki, August 7, 2013,

Helena Laavi

Contents

List of Publications

This thesis consists of an overview and of the following publications which are referred to in the text by their Roman numerals.

I Helena Laavi, Petri Uusi-Kyyny, Juha-Pekka Pokki, Minna Pakkanen, and Ville Alopaeus. Vapor–Liquid Equilibrium for the Systems 2-Methylpropane + Methanol, + 2-Propanol, + 2-Butanol, and + 2-Methyl-2-propanol at 364.5 K. *J. Chem. Eng. Data*, 53 (4) 913–918, March 15, 2008.

II Helena Laavi, Anna Zaitseva, Juha-Pekka Pokki, Petri Uusi-Kyyny, Younghun Kim, and Ville Alopaeus. Vapor–Liquid Equilibrium, Excess Molar Enthalpies, and Excess Molar Volumes of Binary Mixtures Containing Methyl Isobutyl Ketone (MIBK) and 2-Butanol, *tert*-Pentanol, or 2-Ethyl-1-hexanol. *J. Chem. Eng. Data*, 57 (11) 3092–3101, October 15, 2012.

III Aarne T. Sundberg, Helena Laavi, Younghun Kim, Petri Uusi-Kyyny, Juha-Pekka Pokki, and Ville Alopaeus. Vapor–Liquid Equilibria, Excess Enthalpy, and Excess Volume of Binary Mixtures Containing an Alcohol (1-Butanol, 2-Butanol, or 2-Methyl-2-butanol) and 2-Ethoxy-2-methylbutane. *J. Chem. Eng. Data*, 57 (12) 3502–3509, November 5, 2012.

IV Helena Laavi, Juha-Pekka Pokki, Petri Uusi-Kyyny, Alexis Massimi, Younghun Kim, Erlin Sapei, and Ville Alopaeus. Vapor–Liquid Equilibrium, Excess Molar Enthalpies, and Excess Molar Volumes of Binary Mixtures Containing Ethyl Acetate, Butyl Acetate and 2-Butanol at 350

K. *J. Chem. Eng. Data*, 58 (4) 1011–1019, April 1, 2013.

V Helena Laavi, Juha-Pekka Pokki, Petri Uusi-Kyyny, Younghun Kim, and Ville Alopaeus. Vapor–Liquid Equilibrium, Excess Molar Enthalpies, and Excess Molar Volumes of Binary Mixtures Containing 2-Ethoxy-2-methylpropane or 2-Ethoxy-2-methylbutane and Acetonitrile or Propanenitrile. *J. Chem. Eng. Data*, 58 (4) 943–950, March 15, 2013.

Author's Contribution

Publication I: "Vapor–Liquid Equilibrium for the Systems 2-Methylpropane + Methanol, + 2-Propanol, + 2-Butanol, and + 2-Methyl-2-propanol at 364.5 K"

The author processed the data, analyzed the results, and wrote the manuscript.

Publication II: "Vapor–Liquid Equilibrium, Excess Molar Enthalpies, and Excess Molar Volumes of Binary Mixtures Containing Methyl Isobutyl Ketone (MIBK) and 2-Butanol, *tert*-Pentanol, or 2-Ethyl-1-hexanol"

The author measured the excess enthalpy and excess volume data, processed these data, analyzed the results, and wrote the manuscript.

Publication III: "Vapor–Liquid Equilibria, Excess Enthalpy, and Excess Volume of Binary Mixtures Containing an Alcohol (1-Butanol, 2-Butanol, or 2-Methyl-2-butanol) and 2-Ethoxy-2-methylbutane"

The author measured the excess enthalpy and excess volume data, processed these data, and helped in writing the manuscript.

Publication IV: "Vapor–Liquid Equilibrium, Excess Molar Enthalpies, and Excess Molar Volumes of Binary Mixtures Containing Ethyl Acetate, Butyl Acetate and 2-Butanol at 350 K"

The author measured the excess enthalpy and excess volume data, processed the data together with the VLE data, analyzed the results, and wrote the manuscript.

Publication V: "Vapor–Liquid Equilibrium, Excess Molar Enthalpies, and Excess Molar Volumes of Binary Mixtures Containing 2-Ethoxy-2-methylpropane or 2-Ethoxy-2-methylbutane and Acetonitrile or Propanenitrile"

The author measured the excess enthalpy and excess volume data, processed the data together with the VLE data, analyzed the results, and wrote the manuscript.

Notation

Symbols

a	Parameter
B	Second coefficient of the virial equation of state
b	Parameter of the cubic equation of state
C	Third coefficient of the virial equation of state
F	Function
f	Fugacity
G	Gibbs free energy
H	Enthalpy
k	Binary interaction parameter
M	Mixing property
M	Molar mass
N	Total number (of components)
n	Amount of moles
p	Pressure
R	Gas constant 8.31441 $J \cdot K^{-1} \cdot mol^{-}1$
S	Entropy
T	Temperature
V	Calorimetric voltage signal
V	Volume
x	Liquid phase molar fraction
y	Vapor phase molar fraction
z	Compressibility factor
z	Total composition

Greek Letters

α Temperature dependent alpha function in Eq. 2.17
β Parameter in Eq. 2.17
γ Liquid phase activity coefficient
γ Parameter in Eq. 2.17
δ Parameter in Eq. 2.17
κ Isothermal compressibility
Λ Adjustable paramater in Wilson activity coefficient model
λ Adjustable paramater in Wilson activity coefficient model
μ Chemical potential
ρ Density
ϕ Fugacity coefficient
ω Acentric factor

Superscripts

$\circ$ Standard state
∞ Infinite dilution
E Excess
IG Ideal gas
IM Ideal mixture
L Liquid
V Vapor

Subscripts

+	Maximum value
–	Minimum value
c	Critical
calc	Calculated
circ	Circulation still
HS	Headspace
i	Component index
j	Component index
lit	Literature
m	Molar
meas	Measured
mix	Mixture
r	Reduced property (normalized by the fluid's state property at its critical point)
ref	Reference system

Mathematical Notations

d	Derivative
$\ln$	Natural logarithm
$\overline{H}$	Partial molar property of H
$\dot{n}$	Flow of n
$(\,)_T$	Constant T
$\lvert\,\rvert$	Absolute value
F	Function
Δ	Difference between two values
∂	Partial derivative
$\sum$	Sum
$\int$	Integral

Abbreviations and Acronyms

1-BuOH	1-Butanol, CAS nro: 71-36-3
2-BuOH	2-Butanol, CAS nro: 78-92-2
2-EH	2-Ethyl hexanol, CAS nro: 104-76-7
2-PrOH	2-Propanol, isopropyl alcohol, CAS nro: 67-63-0
ACN	Acetonitrile, CAS nro: 75-05-8
BuOAc	Butyl acetate, CAS nro: 123-86-4
EOS	Equation of state
ETBE	Ethyl *tert*-butyl ether, IUPAC name: 2-ethoxy-2-methylpropane, CAS nro: 637-92-3
EtOAc	Ethyl acetate, CAS nro 141-78-6
GC	Gas chromatograph
HOC	Hayden–O'Connell
HS	Headspace
LLE	Liquid–liquid equilibrium
MeOH	Methanol, CAS nro: 67-56-1
MIBK	Methyl isobutyl ketone, IUPAC name: 4-Methyl-2-pentanone, CAS nro: 108-10-1
MTBE	Methyl *tert*-butyl ether, IUPAC name: 2-Methoxy-2-methylpropane, CAS nro: 1634-04-4
NRTL	Nonrandom two-liquid
POY	Poynting correction factor (Eq. 2.33)
PPN	Propanenitrile, CAS nro 107-12-0
SRK	Soave–Redlich–Kwong
t-PnOH	*tert*-Pentanol, IUPAC name: 2-Methyl-2-butanol, CAS nro: 75-85-4
TAEE	*tert*-Amyl ethyl ether, IUPAC name: 2-Ethoxy-2-methylbutane, CAS nro 919-94-8
TAME	*tert*-Amyl methyl ether, IUPAC name: 2-Methoxy-2-methylbutane, CAS nro 994-05-8
TBA	*tert*-Butyl alcohol, IUPAC name: 2-Methyl-2-propanol, CAS nro: 75-65-0
UNIFAC	UNIQUAC functional-group activity coefficients
UNIQUAC	Universal quasichemical
VLE	Vapor–liquid equilibrium
VLEFIT	Program package to obtain parameters in models of activity coefficients from phase equilibrium data [1]

1. Introduction

Multiphase reactors are very versatile and therefore widely used in process industry. Especially, the phenomena over the vapor–liquid phase boundary are crucial for the function of the process. The deviation from the equilibrium between these phases is the driving force for mass transfer. Therefore, there is an obvious need to model this. The presence of several phases, however, makes the modeling task more demanding since the complexity of the system increases.

Process models are vital in chemical industry due to the tightening environmental requirements and legislation that aim at greener chemistry. This objective is not fully reached by emphasizing process development of bio-based or renewable chemicals. In addition, the process models and control need to be lifted on an environmentally higher level. This requires investments on developing more accurate process models. Without precise reactor models, improvement on phase behavior modeling cannot be realized. This part of phase behavior research was earlier studied in the Licentiate's Thesis [2, 3, 4].

To meet the increasing needs of process modeling, accurate thermodynamic data are needed for proper estimation of the phenomena taking place in chemical processes. The models for phase behavior are multiple but the correct models base on precise measured data.

The selection of an appropriate thermodynamic model can be one of the most important decisions for an engineer and tools for this purpose, such as decision trees, have been developed [5]. In this thesis, the models represent a small number of the models currently used in the process industry.

1.1 Thermodynamic Properties

The aim of this work is to provide accurate vapor–liquid equilibrium (VLE) data and models for industrially relevant systems. In order to make the VLE data based model extrapolative beyond the experimental temperature range, also excess enthalpy (H^E) data are provided. H^E brings the temperature dependency to the activity coefficient model as described in chapter 2.4 whereas excess volumes (V^E) give the pressure dependency to the activity coefficient model even though this data with the permitted extension of the pressure range are seldom exploited.

1.2 Systems of Interest

In this work, mainly two criteria were stressed in selecting the chemicals and systems to be studied: the chemicals were considered as examples of typical groups of chemicals commonly used in chemical industry or as options to meet the increasing interest on bio-refinery related components. The available VLE or H^E data on these components and their binary mixtures were also scarce.

The typical groups of chemicals to study were alcohols with alkanes, ethers, ketones, or esters. In addition, examples of binary systems of ethers with nitriles were selected to extend the scope of the study to comprise also compounds other than oxygen containing hydrocarbons.

1.2.1 Alkane with Alcohols

As an alkane, isobutane is widely used chemical in chemical industry e.g. as an propellant, refrigerant, or as a feedstock for petroleum industry. In petroleum industry, isobutane is used as a component of gasoline octane blends, as a refining feedstock for alkylation, and in methyl *tert*-butyl ether (MTBE) and *tert*-amyl methyl ether (TAME) manufacturing processes. In these processes, the presence of alcohols generates a necessity to understand the behavior of the binary systems of isobutane and alcohols.

1.2.2 Ether with Alcohols

2-Ethoxy-2-methylbutane, also known as *tert*-amyl ethyl ether (TAEE), is manufactured from isopentenes, also known as isoamylenes, and ethanol.

Ethanol as well as butanols can be produced from biomass and thus the use of bio-based components in gasoline is promoted [6]. Mixtures consisting of TAEE and alcohols serve as a meaningful and industrially relevant example for studying the manufacturing TAEE [7] and the thermophysical properties of binary mixtures of this ether and alcohols.

1.2.3 Ketone with Alcohols

Methyl isobutyl ketone (MIBK, IUPAC name 4-methyl-2-pentanone) is a widely used solvent in process industry. Alcohols can be used together with MIBK in the solvent phase to improve the results of the extraction process. Therefore, the binary systems of MIBK and some alcohols were selected as a topic to be studied.

1.2.4 Esters with Alcohol

Ethyl acetate (EtOAc) and butyl acetate (BuOAc) are currently considered among promising candidates for bio-based fuel additives since renewable fuels and bio-based fuel additives are gaining more and more attention [8, 9, 10]. This type of chemicals are assumed to cut down the green house gas emissions due to the bio-based origin of the component.

1.2.5 Ethers with Nitriles

ETBE (ethyl *tert*-butyl ether, IUPAC name 2-ethoxy-2-methylpropane) and TAEE are used as fuel oxygenates. Currently, ETBE is along with MTBE one of the most used fuel oxygenate. In the future trendes, the shares of ETBE and TAEE are expected to increase whereas the share of MTBE is expected to decrease [11].

In the manufacturing process of the ethers, the C_4 and C_5 cuts from the catalytic fluid cracking unit contain nitriles that poison the etherification catalyst. Acetonitrile (ACN) and propanenitrile (PPN) are typical examples of these poisons. In addition, ethers easily form azeotropes with nitriles which may cause problems in processes. Therefore, accurate thermodynamic data and models are needed. In addition to the required VLE data measurements, also H^{E} data are needed to generate temperature dependent models for these systems.

2. Thermodynamic Principles

In this chapter, the basic thermodynamic principles of vapor–liquid equilibrium (VLE) and excess enthalpies (H^{E}) are described. In order to accurately describe phase equilibria involving liquid and vapor phases, especially at elevated pressures, deviations from the ideal vapor and ideal liquid usually need to be taken into account.

2.1 Equations of State

The four state variables, pressure p, volume V, amount of moles of the component n, and temperature T, specify the state of a pure gas. However, it has been established experimentally that specifying only three of these variables fixes also the value of the fourth variable. An interrelation of these four variables is an equation of state (EOS) of which the general form is

$$p = f(T, V, n) \tag{2.1}$$

For ideal gases, the gas constant R is used to yield the following equation

$$pV = nRT \tag{2.2}$$

Real gases, however, show deviations from the ideal gas law because molecules interact with each other. To overcome the model discrepancy with real gases, a compressibility factor z is used instead.

$$z = \frac{pV_m}{RT} \tag{2.3}$$

where V_m is the molar volume.

2.1.1 Virial Equation of State

The virial EOS provides a power series form for the compressibility factor z that can be equally expressed as a function of volume, density or pressure [12].

$$z = \frac{pV_m}{RT} = 1 + \frac{B(T)}{V_m} + \frac{C(T)}{V_m^2} + \dots \tag{2.4}$$

where B and C are the second and third temperature dependent coefficients of the virial equation.

Often it is enough to use only the two first terms of the virial EOS. In a mixture of N components, the $B_{ij}(T)$ characterizes the binary interactions between species i and j at composition y [12].

$$B = \sum_{i=1}^{N} \sum_{j=1}^{N} y_i y_j B_{ij}(T) \tag{2.5}$$

2.2 Cubic Equation of State

Cubic equations of state interrelate p, V_m, and T. They are of third degree in volume, as the name indicates. These equations provide another tool for more accurate description of the real gas behavior.

Redlich and Kwong [13] made a substantial improvement for the previously used simple cubic equation of state that had no temperature dependency in the adjustable parameters. They suggested the following form for the equation [12].

$$p = \frac{RT}{V_m - b} - \frac{a}{\sqrt{T} V_m (V_m + b)} \tag{2.6}$$

$$V_m = z\frac{RT}{p} \tag{2.7}$$

$$a = 0.42748 R^2 T_c^{2.5} / p_c \tag{2.8}$$

$$b = 0.08664 R T_c / p_c \tag{2.9}$$

where a and b are adjustable parameters based on the critical properties of the fluid.

Soave [14] modified the temperature-dependent term $a/\sqrt{T}$ of the Redlich–Kwong equation to result in an alpha function $\alpha(T, \omega)$ that was primarily formulated to meet the vapor pressure data of hydrocarbons. The modification involves the acentric factor ω that can be obtained from

the vapor pressure data of the pure component. The Soave modification of the Redlich–Kwong EOS is commonly used due to its good accuracy in relation to the simplicity of the formula.

$$p = \frac{RT}{V_m - b} - \frac{a\alpha}{V_m(V_m + b)} \tag{2.10}$$

$$a = 0.427747 R^2 T_c^2 / p_c \tag{2.11}$$

$$b = 0.08664 R T_c / p_c \tag{2.12}$$

$$\alpha = \left[1 + (0.48508 + 1.55171\omega - 0.15613\omega^2)(1 - T_r^{0.5})\right]^2 \tag{2.13}$$

By assuming quadratic mixing rules the binary interactions between the components of the mixture were assumed symmetric [12].

$$a\alpha = \sum\sum y_i y_j (a\alpha)_{ij} \tag{2.14}$$

$$b = \sum y_i b_i \tag{2.15}$$

$$(a\alpha)_{ij} = (1 - k_{ij})\sqrt{(a\alpha)_i (a\alpha)_j} \tag{2.16}$$

$$k_{ij} = 0 \text{ for hydrocarbon pairs and hydrogen}$$

where k_{ij} is a cross-parameter of molecular interactions.

After Soave, there have been several other modifications to the original form of the cubic equation of state. One general form covering these equations is shown in equation 2.17 [12].

$$p = \frac{RT}{V_m} - \frac{\alpha(T) - \delta(T)/V_m}{(V_m + \beta)(V_m + \gamma)} \tag{2.17}$$

where α, δ, β, and γ are adjustable parameters. Usually, only α and δ depend on temperature.

2.3 Vapor–Liquid Equilibrium

In phase equilibrium, the Gibbs free energies in the coexisting phases are equal as shown in equation 2.18.

$$G^L = G^V \tag{2.18}$$

where G^L and G^V are the liquid and vapor Gibbs free energies.

Fugacity, f, describes the deviation from the ideal gas law [15].

$$f = p \exp\left\{\frac{G - G^{IG}}{RT}\right\} = p \exp\left\{\frac{1}{RT}\int_0^p \left(V - \frac{RT}{p}\right) dp\right\} \tag{2.19}$$

where the superscript IG denotes ideal gas behavior, V is volume. From the equation 2.19 it follows that in vapor–liquid equilibrium (VLE) the Gibbs free energies are equal and the fugacities of the phases are equal.

$$f_i^V = f_i^L \tag{2.20}$$

Fugacities can be expressed by using fugacity coefficients, $\phi = f/p$. In mixtures, the vapor phase composition and pressure are needed to determine the vapor phase fugacity as shown in equation 2.21.

$$f_i^V = \phi_i^V y_i p \tag{2.21}$$

For liquid phase fugacities, either the liquid phase fugacity coefficients ϕ_i^L or the liquid phase standard state fugacity coefficients ϕ_i° can be used (see equations 2.22 and 2.23). The standard state (marked with $^\circ$) denotes the saturated state of the pure liquid at the system temperature and pressure.

$$f_i^L = \phi_i^L x_i p \tag{2.22}$$

$$f_i^L = \gamma_i x_i p_i^\circ \phi_i^\circ \cdot \mathrm{POY} \tag{2.23}$$

where the POY is the Poynting correction (see equation 2.33).

Activity coefficients, γ_i, are used for liquid mixtures that are not describable by an equation of state. An activity coefficient is a function of temperature, pressure, and composition as shown in equation 2.24

$$\overline{f}_i^L = x_i \gamma_i f_i^{\circ,L} \tag{2.24}$$

where the overbar denotes partial molar property and the superscript $^\circ$ denotes the standard state. The activity coefficients depend on the Gibbs free energy as shown in the equation 2.25.

$$\gamma_i = \exp\left(\frac{\overline{G}_i^E}{RT}\right) \tag{2.25}$$

2.4 Excess Properties

Excess properties, M^{E}, describe how the mixing of real fluids deviate from the mixing of ideally behaving fluids.

$$M^{E} = \Delta M_{\text{mix}} - \Delta M_{\text{mix}}^{IM} = \sum_i x_i \overline{M}_i - \sum_i x_i \overline{M}_i^{IM} = \sum_i x_i \left(\overline{M}_i - \overline{M}_i^{IM} \right) \tag{2.26}$$

where the superscript IM denotes ideal mixture.

Excess enthalpy, H^{E}, and excess volume, V^{E}, are the temperature and pressure derivatives of the Gibbs free energy, G^{E}.

$$\left(\frac{\partial(\frac{G^{E}}{T})}{\partial T} \right)_P = -\frac{H^{E}}{T} \tag{2.27}$$

$$\left(\frac{\partial(\frac{G^{E}}{T})}{\partial P} \right)_T = \frac{V^{E}}{T} \tag{2.28}$$

The equation 2.27 is also called the Gibbs-Hemholtz equation. Combined with the equation 2.25, the H^{E} and V^{E} can be used in estimating the temperature and pressure dependency of the activity coefficients.

Temperature dependency of the activity coefficients shows the relation between excess partial molar enthalpy $\overline{H}^{\mathrm{E}}$ and activity coefficients [15]

$$\gamma_i(T_2, p, x) = \gamma_i(T_1, p, x) \exp\left[-\int_{T_1}^{T_2} \frac{\overline{H}^{E}(T, p, x)}{RT^2} \right] \tag{2.29}$$

If the temperature dependence of the excess enthalpy is negligible, the equation 2.29 becomes

$$\gamma_i(T_2, p, x) = \gamma_i(T_1, p, x) \exp\left[-\int_{T_1}^{T_2} \frac{\overline{H}^{E}(x)}{R} \left(\frac{1}{T_2} - \frac{1}{T_1} \right) \right] \tag{2.30}$$

The pressure dependency of the activity coefficients can be expressed by using excess partial molar volume $\overline{V}^{\mathrm{E}}$ [15]

$$\gamma_i(T, p_2, x) = \gamma_i(T, p_1, x) \exp\left[\int_{p_1}^{p_2} \frac{\overline{V}^{E}(T, p, x)}{RT} dp \right] \tag{2.31}$$

If the pressure dependency of $\overline{V}^{\mathrm{E}}$ is negligible the equation 2.31 becomes

$$\gamma_i(T, p_2, x) = \gamma_i(T, p_1, x) \exp\left[\frac{\overline{V}^{E}(T, x)(p_2 - p_1)}{RT} \right] \tag{2.32}$$

The exponential term in equation 2.31 is often called the Poynting correction factor (POY). It expresses the liquid volume dependency on pressure. At moderate pressues the value of the factor is very close to unity [12].

$$(\mathrm{POY}) = \exp\left[\int_{p^{\circ}}^{p} \frac{\overline{V}^{E}(T, p, x)}{RT} dp \right] \tag{2.33}$$

where the superscript $^{\circ}$ denotes saturated state of the vapor pressure.

3. Modeling

In this chapter, the modeling principles of the measured thermodynamic properties are presented. First, the used fugacity and activity coefficient models are presented. Second, the data reduction procedure [16] is presented. Third, the used data regression program called VLEFIT [1] with the used objective functions is briefly outlined. Finally, the principles of the used data consistency tests are described.

3.1 Vapor Phase Fugacity Coefficient Models

The variety of available vapor phase fugacity coefficient models is wide so criteria for the selection of the appropriate model are required. As a general rule, the chosen model should not be too complicated, too simple, or intended for totally different types of systems in respect of the experimental data.

In this work, the vapor phase fugacities were calculated by using the SRK equation of state 2.10 with quadratic mixing rules in the publication I. In other publications II, III, IV, and V, the Hayden–O'Connell (HOC) method with the chemical theory [17, 18] was used. In addition, in the publication IV, the assumption of ideal vapor and ideal liquid was also utilized in comparative evaluation of the VLE data consistency of the binary system of ethyl acetate and butyl acetate.

3.1.1 Hayden–O'Connell Method and the Chemical Theory

The Hayden–O'Connell (HOC) method [17, 18] is based on a theory of molecular interactions. It is one method among the others to predict the second virial coefficients for the virial equation of state (equation 2.4). The power of the HOC method is in its good accuracy in relation to its simplicity. The HOC method predicts the coefficients only by using the critical

properties and molecular parameters, and, if appropriate, including association parameters. All these properties may usually be estimated from molecular structure to the required accuracy.

The chemical theory is especially recommended in the modeling of components, such as carboxylic acids, that form dimers in solutions. This type of components can often be present in wood based feedstock that is to be refined to produce e.g. renewable fuels or fine chemicals.

In binary mixtures, the theory postulates that there is a dimerization equilibrium described in equation 3.1

$$i + j \rightleftarrows ij \tag{3.1}$$

where i and j are the two monomer molecules that may or may not be chemically identical. Chemical equilibrium can be written for the dimer ij formation by using a chemical equilibrium constant. Monomer i belongs to species i and monomer j to species j.

3.2 Liquid Phase Activity Coefficient Models

For mixtures for which equations of state models are inapplicable, attemps to estimate G^{E} are made empirically or semitheoretically as shown in previous chapter 2 in equation 2.25.

Both the Wilson [19] and the NRTL [20] models are based on the same type assumption on molecular level [15]. That is to say, around each chosen molecule there is a local composition. However, the factors affecting the molecular-level behavior vary. These include among others the bulk composition, the size of the molecules, and the energy of interaction of the surrounding molecules in relation to the chosen molecule.

3.2.1 The Wilson Activity Coefficient Model

The Wilson model [19] has often shown superior performance in comparison to other activity coefficient models [12]. The Wilson activity coefficient model has two adjustable parameters, lambdas. Originally, the big lambdas, Λ were used and they can be described by the temperature dependent small lambdas, λ. For a binary mixture, Λ and λ are defined as shown in equations 3.2–3.5.

$$\Lambda_{12} = \frac{V_{m,2}^L}{V_{m,1}^L}\exp\left(-\frac{\lambda_{12}}{RT}\right) \quad (3.2)$$

$$\Lambda_{21} = \frac{V_{m,1}^L}{V_{m,2}^L}\exp\left(-\frac{\lambda_{21}}{RT}\right) \quad (3.3)$$

$$\lambda_{12} - \lambda_{11} = a_{0,12} + a_{1,12}T + a_{2,12}T^2 \quad (3.4)$$

$$\lambda_{21} - \lambda_{22} = a_{0,21} + a_{1,21}T + a_{2,21}T^2 \quad (3.5)$$

where $a_{0,ij}$, $a_{1,ij}$, and $a_{2,ij}$ are parameters giving the temperature dependency to the adjustable parameters, λ_{ij}.

3.2.2 The NRTL Activity Coefficient Model

The NRTL (nonrandom two-liquids) model [20] is also a two-parameter model like the Wilson model [19]. The difference is in the stressing of the mole fractions.

3.2.3 The UNIQUAC Activity Coefficient Model

The UNIQUAC (UNIversal QUAsiChemical) model [21] is based on statistical thermodynamics. It approximates the interactions of the molecular surfaces.

3.2.4 The UNIFAC (Dortmund) Activity Coefficient Model

The UNIFAC (UNIQUAC Functional-group Activity Coefficients) model [22] is an extension of the UNIQUAC model. It is a semi-empirical predictive method to estimate the ativity coefficients based on functional groups of the molecules.

3.3 The Method of Total Pressure Data Reduction

The used method for the total pressure data reduction [16] describes a procedure based on least squares how to obtain activity coefficients from total pressure VLE data. The total pressure can be expressed as a function of partial pressures. For component vapor pressures, activity coefficient expressions are needed. In publication I, highly flexible Legendre polynomials [23] were used to model the total pressure VLE data together with the data reduction procedure.

In this method, the measured p, T, n_1, and n_2 were reduced into phase equilibrium data by equating the fugacities of the vapor and the liquid

phases as shown in equation 3.6.

$$\frac{y_i}{x_i} = \frac{\gamma_i \phi_i^\circ p_i^\circ}{\phi_i p} \exp \int_{p_i^\circ}^{p} \frac{V_{m,i}^L}{RT} dp \tag{3.6}$$

where x_i and y_i are the liquid and vapor compositions, γ_i is the liquid phase activity coefficient, ϕ_i vapor phase fugacity coefficient, $V_{m,i}^L$ is the liquid molar volume, R is the universal gas constant, and T is temperature. The superscript $^\circ$ denotes saturated state of vapor pressure.

In the data reduction, in order to calculate x_i and y_i, the Legendre polynomials [23] were used for the calculation of liquid phase activity coefficients, and the Soave–Redlich–Kwong (SRK) [14] equation of state with quadratic mixing rules for the vapor phase fugacities. The binary interaction parameters were set to zero. The liquid molar volumes in the Poynting correction were calculated by using the Rackett equation [24].

The procedure to optimize the Legendre parameters follows the one suggested by Pokki [25] so as to avoid overfitting. The number of used parameters was increased one by one until no remarkable decrease in the residual was observed. This was considered as the criterion for selecting the appropriate number of the parameters.

3.4 The VLEFIT Program Package

VLEFIT is a program package through which the parameters of activity coefficient models can be optimized based on thermodynamic data [1]. It contains various options to compute values of the thermodynamic functions needed in the calculation of e.g. VLE, liquid–liquid equilibrium (LLE), and activity coefficients.

The program accepts various experimental data such as VLE, H^E, and LLE data. The input may consist of several data sets of the same type of data at separate conditions as well as different types of data sets. The user selects the appropriate methods how to calculate pure component properties and also the fugacity coefficient and activity coefficient model for the components for the system. When the thermodynamic model functions are selected the program optimizes the parameters of the model based on the selected objective functions that are explained next in chapter 3.4.1.

3.4.1 Objective Functions

The purpose of using objective functions is to reproduce the given experimental data by minimizing the deviations between the model and the experimental data. The objective functions are usually defined as the deviations between the measured quantities and the modeled quantities. There are various ways to select the thermodynamic properties for this purpose. In the case of VLE and H^E data, the most commonly selected ones are the deviations of pressure, Δp; activity coefficients, $\Delta\gamma$; vapor mole fractions, Δy; or excess enthalpies, ΔH^E.

In this work, the used objective functions were the squares of the relative deviations of the above mentioned thermodynamic properties, p, γ, y, and H^E. The equation 3.7 shows the typical objective function for pressure

$$F = \sum_{i=1}^{NP} \left(\frac{(p_{\text{calc},i} - p_{\text{meas},i})}{p_{\text{meas},i}} \right)^2 \tag{3.7}$$

where NP is the number of experimental points.

3.5 Data Consistency

The experimental data should be tested for thermodynamic consistency that reveals the quality of the data. The Gibbs–Duhem equation relates the chemical potentials, μ, of the components in a mixture:

$$-SdT + VdP = \sum x_i d\overline{G}_i = \sum x_i d\mu_i \tag{3.8}$$

where S is entropy.

At constant T and p

$$\sum x_i d\mu_i = 0 \tag{3.9}$$

$$\sum x_i d\gamma_i = 0 \tag{3.10}$$

The significance of the Gibbs–Duhem equation is that the chemical potential of a component in a mixture cannot change independently of the the chemical potentials of the other components [26].

For binary mixtures holds

$$x_1 \frac{\partial \gamma_1}{\partial x_1} + x_2 \frac{\partial \gamma_2}{\partial x_1} = 0 \tag{3.11}$$

From the equation 3.11 follows that

1. The slopes $d\gamma_i/dx_1$, are equal but of opposite signs at equal molar fractions x_1 = x_2 = 0.5.

2. The slope of γ_1 is zero at x_1 = 1, and that of γ_2 is zero at x_1 = 0.

3. The area (integral) test can be developed from the equation 3.11. For consistent thermodynamic data, the area should be close to zero. In case the data is not truly isothermal or isobaric, small deviations from zero are allowed even though pressure usually has little effect on liquid phase behavior.

Three consistency tests were used in this work for the $xyTP$ data: the area test, the point test, and the infinite dilution test [27, 28, 29, 23]. The area test suitable for the HS-GC xyT data was used [30]. Since the pure component GC peak areas were very unstable, correlations based on the binary mixture areas were used for pure component areas [31].

3.5.1 The Area Test

The principle of the area test is to fulfill the Gibbs–Duhem equation by taking the integral over the composition range. For binary systems, another form for the Gibbs–Duhem equation 3.11 is the following which is widely used basis for consistency test of experimental data.

$$x_1 d\ln\gamma_1 + x_2 d\ln\gamma_2 = -\frac{H^{\mathrm{E}}}{RT^2}dT + \frac{V^{\mathrm{E}}}{RT}dP \tag{3.12}$$

At constant temperature and pressure the equation 3.12 becomes

$$x_1 d\ln\gamma_1 + x_2 d\ln\gamma_2 = 0 \tag{3.13}$$

By taking a derivative of the equation 3.12

$$\begin{aligned} d\left(\frac{G^{\mathrm{E}}}{RT}\right) &= d(x_1 d\ln\gamma_1 + x_2 d\ln\gamma_2) \\ &= (x_1 d\ln\gamma_1 + x_2 d\ln\gamma_2) + \ln\gamma_1 dx_1 - \ln\gamma_2 dx_1 \end{aligned} \tag{3.14}$$

The group in the parantheses is zero by equation 3.13. The excess Gibbs energy is zero at the both ends of the composition range. Therefore the integral of the remaining part of the equation 3.14 results in

$$\int_0^1 d\left(\frac{G^{\mathrm{E}}}{RT}\right) = \int_0^1 (\ln\gamma_1 - \ln\gamma_2)dx_1$$

$$= \int_0^1 \ln\frac{\gamma_1}{\gamma_2} dx_1 = 0 \tag{3.15}$$

The equation 3.15 is used as the area test. The criterion for passing the test is that for the area A holds: $A < 0.03$.

3.5.2 The Infinite Dilution Test

Under the conditions of infinite dilutions, the following relationships should be satisfied:

$$\left(\frac{\frac{G^{\mathrm{E}}}{RT}}{x_1 x_2}\right)_{x_1=0} = \left(\ln\frac{\gamma_1}{\gamma_2}\right)_{x_1=0} = \left(\ln\gamma_1\right)_{x_1=0} = \ln{\gamma_1}^{\infty} \tag{3.16}$$

$$\left(\frac{\frac{G^{\mathrm{E}}}{RT}}{x_1 x_2}\right)_{x_2=0} = \left(\ln\frac{\gamma_2}{\gamma_1}\right)_{x_2=0} = \left(\ln\gamma_2\right)_{x_2=0} = \ln{\gamma_2}^{\infty} \tag{3.17}$$

That is the values of $\frac{\frac{G^{\mathrm{E}}}{RT}}{x_1 x_2}$ and infinite dilution activity coefficients ${\gamma_i}^{\infty}$ should coincide [27]. The criterion for the test is presented in equation 3.18.

$$\text{criterion at infinite dilution: } \frac{\frac{\frac{G^{\mathrm{E}}}{RT}}{x_1 x_2}}{\ln\frac{\gamma_1}{\gamma_2}} < 30 \tag{3.18}$$

3.5.3 The Point Test

The point test compares the deviations between the measured experimental points and the calculated points. Examination of the data point by point avoids mutual cancellation of individual errors.

In this work, the vapor phase compositions were selected as the target property for the test Δy = y_{exp} - y_{calc}. The criterion for passing the point test was that the average deviation should be less than 0.01. [23]

4. Experimental Procedures

Thermodynamic data can be obtained by using various equipment and experimental procedures. In this work, three different experimental setups, static total pressure apparatus, circulation still, and headspace–gas chromatograph, were utilized for VLE measurements. A SETARAM C80 calorimeter was applied to excess enthalpy measurements and a vibrating tube density measuring cell was used in excess volume measurements.

The measured data, however, are of less value if the experimental uncertainties are not reported. In this chapter, the used equipment and the experimental procedures are first described and then the experimental uncertainties are reported.

4.1 Static Total Pressure Apparatus

The static total pressure apparatus was applied to measuring the VLE of the binary mixtures of isobutane and alcohols. The simplified scheme of the equipment is shown in figure 4.1. The apparatus consisted of an equilibrium cell with a magnetic stirrer. The volume of the cell was 112.68 cm^3 and the cell was submerged into a thermostated water bath. Details of the apparatus are explained in Uusi-Kyyny *et al*. [32] and in Hynynen *et al*. [33].

In this type of system, the data obtained from the system comprises the total pressure p, temperature T, and the amount of the two components n_1 and n_2 inserted into the system. The vapor and liquid phase compositions were not measured directly but they were obtained through the total pressure data reduction [16] as explained in chapter 3.3. This makes it crucial to ensure that the used liquid is properly degassed under vacuum and contains no dissolved gasses since the amount of dissolved gasses in the liquid significantly depends on the pressure.

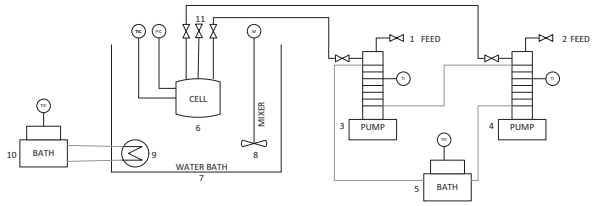

Figure 4.1. Static total pressure apparatus: (1),(2) Feeds; (3),(4) ISCO syringe pumps; (5) Thermal bath for the feed pumps; (6) Equilibrium cell; (7) Water bath for the equilibrium cell; (8) Mixer of the water bath; (9) Heat exchanger; (10) Thermal bath to control the temperature of the water bath of the equilibrium cell; (11) Outlet from the equilibrium cell to the vacuum line.

4.1.1 Experimental Procedure of the Static Total Pressure Apparatus

The details of the experimental procedure of measuring VLE with the static total pressure apparatus are given in [34] and only a brief overview is given here. In the experiments, one of the components (isobutane) was first fed into the cell by using an ISCO syringe pump. Next, the second component was gradually fed to the system by using another ISCO syringe pump. After each insertion, the pressure and the temperature of the system were recorded as well as the volume of the freshly added component. The experiments were planned such that at the end of the experiments, when the cell was full, the composition in the cell was approximately equimolar. Then, the cell was emptied and the whole procedure was repeated from the other end of the composition range. It was considered as an indication of good data quality if the measured vapor pressures at the equimolar composition coincided.

4.2 Circulation Still

The circulation still of Yerazunis type [35] was utilized in measuring VLE of binary systems in publications II, III, IV, and V. A simplified scheme of the used equipment is shown in figure 4.2. The liquid required for running the apparatus was approximately 80 cm^3. A stainless steel container was added between the equilibrium cell and the vacuum pump to stabilize the pressure. The use of this type of equipment was limited to subatmospheric pressures. Details of the used equipment can be found in references [36, 37].

4.2.1 Experimental Procedure of the Circulation Still

The procedure is described in detail in [37]. Pure component 1 was first introduced into the circulation still, and its vapor pressure was measured. Next, the second component was added and approximately after 30 min a constant temperature was re-reached. Then, after (30 to 45) min the values were recorded by taking simultaneous samples from the liquid phase and condensed vapor phase chambers. A part of the sample was analyzed with a gas chromatoghaph (GC) and the remaining part of the sample was used for refractive index measurement for comparison.

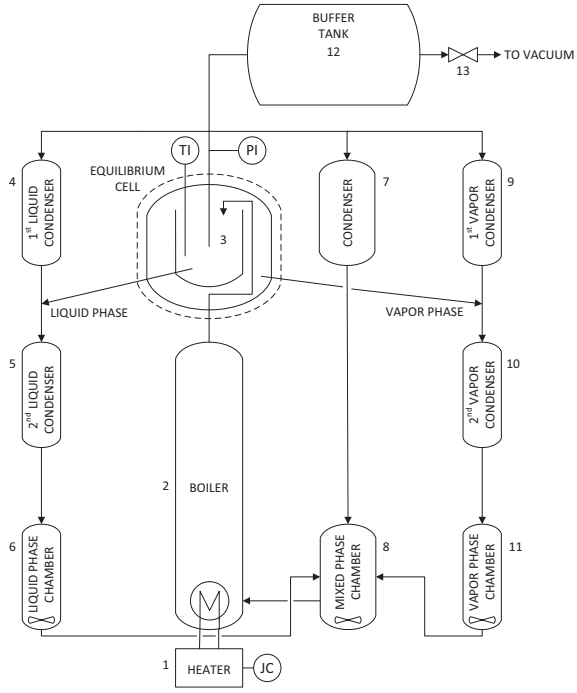

Figure 4.2. Circulation still: (1) Heating source; (2) Immersion heater; (3) Insulated equilibrium cell; (4) First liquid phase condenser; (5) Second liquid phase condenser; (6) Condensed liquid phase chamber with a magnetic stirrer; (7) Condenser for the circulating mixture from the equilibrium cell; (8) Mixing chamber with a magnetic stirrer; (9) First vapor phase condenser; (10) Second vapor phase condenser; (11) Condensed vapor phase chamber with a magnetic stirrer; (12) A stainless steel container for stabilizing the pressure; (13) Adjusting valve for the pressure control.

4.3 Headspace–Gas Chromatograph (HS-GC)

Headspace–gas chromatograph (HS-GC) technique was used for measuring VLE of binary systems containing methyl isobutyl ketone (MIBK) and some alcohols. The technique is suitable for systems containing even solid contaminants as it takes samples only from the gas phase. HS-GC is most commonly used for high-ppb to percent concentration ranges, such as determining of volatile organic components in water, fragrance analysis, and VLE or LLE studies with or without addition of salts [30].

HS-GC can be used only for temperatures higher than room temperature and moderately higher pressures than atmospheric pressure due to the used glass vials and the fact that the equipment is open to atmospheric pressure and room temperature. A full data set is not obtained since the equilibrium pressure is not measured due to the fact that the gas phase sample is diluted with air. The equilibrium temperature T, liquid molar fractions x_i, and vapor molar fractions y_i are determined.

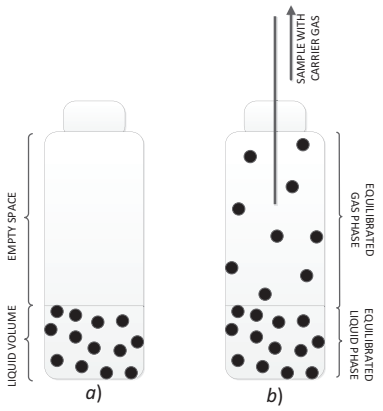

Figure 4.3. HS sampling: a) Gravimetrically prepared HS sample vial with liquid phase and gas phase volumes; b) Equilibrated HS sample vial and perforated septum cap to transfer the sample through the needle to GC.

4.3.1 Experimental Procedure of the HS-GC

Agilent Technologies 7697A headspace sampler was used together with Agilent 6890N gas chromatograph (GC) for the vapor phase sample analysis. The samples of the binary systems were gravimetrically prepared in 20 cm^3 HS vials. The liquid sample occupied approximately 25 % of the total volume of the vial to ensure a sufficient volume for the gas phase. The sample was taken from the equilibrated gas phase as illustrated in

figure 4.3. The vials were let to equilibrate at the set temperature in the HS oven for at least 30 min prior to sampling. The sampling system was pressurized with helium at 160 kPa absolute pressure.

4.4 Comparison of the VLE Measurement Techniques

In this work, three apparatuses were used in the VLE measurements. In the publication II, two apparatuses were used in parallel for the same binary systems. This was partly used to widen the scope of the experiments and to ensure the high quality of the data.

The three VLE measurement techniques are here briefly compared. First, the suitable operating conditions of the apparatuses are presented. Then, the types of data obtained by using each apparatus are summarized. Finally, the ease of the use of each apparatus is evaluated.

4.4.1 Comparison of the Experimental Conditions

The specifications of the presented equipment are presented in table 4.1. As seen in the table, the main benefit of the static total pressure apparatus was the widest pressure range combined with a relatively wide temperature range. As for the circulation still, the highest temperatures could be reached in comparison to the static apparatus and the HS-GC even though the pressures were limited to subatmospheric pressures. The use of the HS-GC was limited to atmospheric pressure.

Table 4.1. Specifications of the Experimental Equipment.

	Data	T_{min} K	T_{max} K	p_{min} kPa	p_{max} kPa
Static apparatus	zTp	283	368	∼0	2000
Circulation still	$xyTp$	308	473	∼10	∼101
HS-GC	xyT	303	368	∼101	∼101

The ambient temperature of the circulation still was the room temperature that set the lower limit for the temperature range. In order to be able to control the temperature, the equipment had to operate at higher temperature than the ambient temperature. Similarly, the HS-GC was also operated at room temperature so the temperature of the HS-GC oven needed to be higher than 298 K in order to achieve controllability for the temperature.

The lower and upper limits of the temperature and pressure ranges could sometimes be extended by suitable replacements of the parts. For example, the static total pressure apparatus could stand temperatures higher than 368 K in case the water in the thermal bath was replaced by oil that could be heated up to 473 K. However, in order to operate at higher temperature, also the pressure transducer should be replaced with the one that tolerates temperatures higher than 398 K. The valves and tubing of the static total pressure apparatus would bear pressures up to 160 bar but over the whole pressure range, various pressure gauges should be used for narrower pressure ranges. Equilibrium cell set the upper limit for the pressure.

4.4.2 Comparison of Obtainable Data

Only the circulation still provided a full $xyTp$ set of VLE data. This enabled wide processing of the data through e.g. consistency tests.

The static total pressure apparatus provided the total composition data zTp which required data reduction to obtain component mole fractions. Since the compositions were defined through the total pressure, the pressure measurements needed to be performed with extreme care. This was why the degassing of the liquid components was crucial.

The HS-GC provided xyT VLE data. The equilibrium pressure was not defined since the samples were diluted with air and pressurized by the carrier gas.

4.4.3 Comparison of the Ease of the Experiments

The main benefits of the static total pressure apparatus were the wide ranges of temperature and pressure in addition to the simplicity of the experiment. The main drawback was the lack of individual composition data. In addition, the static total pressure apparatus was not suitable for reactive systems.

The main advantage of the circulation still was that both the vapor and the liquid phase samples could be analyzed. Even though a full set of *xyTp* VLE data was obtained, the use of the circulation still was limited by the difference in the boiling points and viscosities of the components [36]. Too high differences in these properties make the boiling unstable and reduces the accuracy of the method.

The HS-GC VLE experiment procedure was rapid, accurate, and easily

automated. However, the potential of this technique was not fully developed yet [30]. The equilibration time, sample volume, and response factors needed to be adjusted to ensure the reliability of the results [30].

4.5 SETARAM C80 Flow Calorimeter

Excess enthalpies (H^{E}) were measured with a SETARAM C80 flow calorimeter with a flow mixing cell [38]. The scheme of the system is shown in figure 4.4. The chemicals were fed into the calorimeter by using two syringe pumps (ISCO 260D, ISCO 500D). The calorimeter was calibrated by using two well-known chemical reference systems: cyclohexane-hexane and methanol-water [39]. This was considered as a recommended calibration procedure for this type of equipment [39, 40].

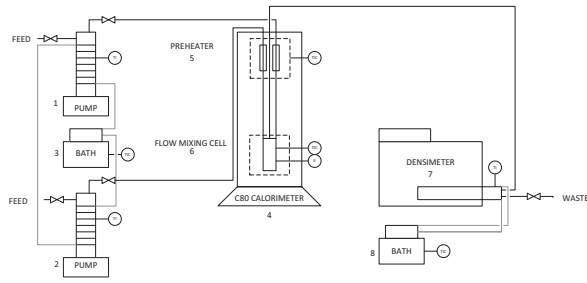

Figure 4.4. SETARAM C80 calorimeter and DMA 512P densimeter: (1) ISCO 500D syringe pump; (2) ISCO 260D syringe pump; (3) Lauda E200 thermal bath for controlling the temperature of the ISCO pumps; (4) SETARAM C80 calorimeter; (5) Preheater; (6) Flow mixing cell; (7) DMA 512P densimeter; (8) Lauda E200 thermal bath for controlling the temperature of the densimeter.

4.5.1 Experimental Procedure of the SETARAM C80 Flow Calorimeter

The procedure is described in detail in publication II. The ISCO pumps were let to equilibrate for 1 hour prior launching the experiments. The total flow rate of the feeds was kept at 0.5 $\mathrm{cm^3 \cdot min^{-1}}$ by varying the pure component flow rates throughout the composition range. After a constant signal was obtained, which took approximately 15 min depending on the system, additional (10 to 15) min were waited to ensure stabilized values to be recorded.

4.6 DMA 512 P Density Measuring Cell (Anton Paar)

A vibrating-tube Antor Paar DMA 512 P densimeter was used for measuring the densities from which the excess volumes were derived. The densimeter was calibrated by using deionised and degassed water [41] and dry air [42] reference systems.

4.6.1 Experimental Procedure of the DMA 512 P Density Measuring Cell

The densimeter was connected to the outlet of the calorimeter unit so that the densimeter signal was also used to check the state of the mixing in calorimeter as can be seen in figure 4.4. In case of incomplete mixing the densimeter signal fluctuated extensively whereas in the case of complete mixing the signal was stable.

The densimeter was thermostated by using a Lauda E200 water immersion thermostat that was set on one hour prior to the measurements. The stabilization of the signal took approximately 10 min at the constant flow rate of 0.5 $cm^3 \cdot min^{-3}$.

4.7 Uncertainties

A clear documentation of the uncertainties of the measured properties is a substantial part of a high quality data set. This thesis contains a significant amount of new experimental data. Only a brief summary of uncertainty estimation is presented here since more detailed descriptions of the uncertainties are provided in the publications.

4.7.1 Uncertainties in the Data of the Static Total Pressure Apparatus

A summary of the uncertainty analysis of the variables in the static total pressure apparatus is presented in table 4.2. The uncertainties of the measured p and T were estimated based on the known uncertainties of the instruments. However, the total composition z was a derived property of which the uncertainty needed to be estimated through calculation. A theoretical maximum uncertainty was derived by using the total differential of the injected amount of moles resulting equation 4.1.

$$\Delta n_1 = n_1 \left(\frac{\Delta \rho_1}{\rho_1} + \frac{1}{\rho_1} \left| \frac{\mathrm{d}\rho_1}{\mathrm{d}T} \right| \Delta T + \kappa_1 \Delta p + \frac{\Delta V_1}{V_1} \right) \tag{4.1}$$

where

$$\kappa_1 = -\frac{1}{V_1} \left(\frac{\mathrm{d}V_1}{\mathrm{d}p} \right)_T \tag{4.2}$$

Then, the total differential of the total concentration z_i was derived as presented in [33, 43] to yield equation 4.3

$$\begin{aligned} \Delta z_1 \quad = \quad & \frac{n_1 n_2}{(n_1 + n_2)^2} \left[\left(\frac{\rho_1}{n_1 M_1} + \frac{\rho_2}{n_2 M_2} \right) \Delta V + \frac{\Delta \rho_1}{\rho_1} + \frac{\Delta \rho_2}{\rho_2} + \right. \\ & \left. \left| \frac{1}{\rho_1} \left(\frac{\mathrm{d}\rho_1}{\Delta T} \right) - \frac{1}{\rho_2} \left(\frac{\mathrm{d}\rho_2}{\Delta T} \right) \right| \Delta T + |\kappa_1 - \kappa_2| \Delta p \right] \end{aligned} \tag{4.3}$$

Table 4.2. Summary of the Uncertainty Analysis of the Variables in the Experiments of the Static Total Pressure Apparatus.

	Description	Type	Uncertainty	Ref.
p	Equilibrium pressure	Measured	Instrument	I
T	Equilibrium temperature	Measured	Instrument	I
n_i	Injected amount of moles	Calculated	Eq. 4.1	I
z_i	Total equilibrium composition	Calculated	Eq. 4.3	I
x_i	Equilibrium composition	Calculated	Eq. 4.4	I
γ_i	Activity coefficient	Calculated	Eq. 4.4	I

Uncertainties for the vapor and liquid phase compositions and for the activity coefficients were approximated by performing the data reduction procedure in the VLEFIT [1] program using upper and lower boundary values for p, T, and n_i. Thus, 16 combinations of theoretical maximum errors were obtained. An average absolute error (see equation 4.4) was reported in the publication. Details of the procedure are found in publication I and in references [43, 33].

$$\Delta x = \max\Big(|x - x_-|, |x - x_+| \Big) \tag{4.4}$$

4.7.2 Uncertainties in the Data of the Circulation Still

A circulation still was used in publications II, III, IV, and V. The measured variables of the circulation still experiments were pressure p, temperature T, and composition x_i, y_i. The pressure and temperature uncer-

tainties were approximated based on the reported uncertainties of the instruments. The uncertainties of the liquid and vapor phase compositions were analyzed by GC, of which the accuracy was defined by the equipment. The repeatability of the sampling at the same composition was not possible since the composition of the circulating fluid changed after each sampling. Nevertheless, identical GC analyses were achieved from parallel runs of one sample.

Table 4.3. Summary of the Uncertainty Analysis of the Variables in the Experiments in the Publications II, III, IV, and V.

	Description	Type	Uncertainty	Ref.
p_{circ}	Equilibrium pressure	Measured	Instrument	II, IV, V
T_{circ}	Equilibrium temperature in circulation still	Measured	Instrument	II, III,IV, V
T_{HS}	Equilibrium temperature in HS-GC	Measured	Instrument	II
x_i, y_i	Equilibrium composition	Measured	Analytics	II, III, IV, V
H^{E}	Excess enthalpy	Calculated	Eq. 4.6	II, III, IV, V
V^{E}	Excess volume	Calculated	Eq. 4.12	II, III, IV, V

4.7.3 Uncertainties in the Data of the HS-GC

In HS-GC measurements, the liquid and gas phase compositions x_i and y_i, and the equilibrium temperature T were measured. The accuracy of the composition was based on the accuracy of the used gas chromatograph and the repeatability of the sample analysis. For the calibration, samples for determining the response factors were prepared as suggested in literature [44]. The accuracy of the temperature was based on the accuracy reported in the manual.

4.7.4 Uncertainties in the Data of the Calorimeter

The uncertainty of the reading of the calorimeter signal was determined by using two well-known chemical reference systems: cyclohexane-hexane

and methanol-water [39]. First, the calorimeter sensitivity parameter, K, was determined by using cyclohexane-hexane binary system as recommended in (see equation 4.5) [38].

$$K = \frac{V_{\text{mix}} - V_{\text{baseline}}}{H^{\text{E}}_{\text{lit}} \dot{n}} \tag{4.5}$$

where V_{mix} is the calorimeter signal for the mixture in μV, V_{baseline} is the calorimeter signal caused by the baseline, $H^{\text{E}}_{\text{lit}}$ is the excess enthalpy reported in literature, and $\dot{n}$ the total molar flow through the calorimeter flow mixing cell.

Then, the accuracy of the calorimeter was checked by using the methanol-water binary system. Furthermore, the effect of varying flow rate ratios from the feed pumps was also considered and substracted from the signal [40]. The uncertainty of H^{E} was then calculated as the average absolute deviation between the calculated H^{E} values obtained by using separately each of the two reference systems.

$$\Delta H^{\text{E}} = \sum_{i=1}^{N} \frac{H^{\text{E}}_{\text{i,ref1}} - H^{\text{E}}_{\text{i,ref2}}}{N} \tag{4.6}$$

4.7.5 Uncertainties in the Data of the Densimeter

The excess volumes were derived from the density data. The total differential was used to estimate the uncertainty. In the following equations, the estimated uncertainties of single variables affecting V^{E} are presented.

$$x_1 = \frac{\frac{\dot{V}_1}{V_{1,m}}}{\frac{\dot{V}_1}{V_{1,m}} + \frac{\dot{V}_2}{V_{2,m}}} \tag{4.7}$$

$$\Delta x_1 = \frac{\frac{\Delta\dot{V}_1}{V_{1,m}} \cdot \left(\frac{\dot{V}_1}{V_{1,m}} + \frac{\dot{V}_2}{V_{2,m}}\right) - \frac{\dot{V}_1}{V_{1,m}} \cdot \left(\frac{\Delta\dot{V}_1}{V_{1,m}} + \frac{\Delta\dot{V}_2}{V_{2,m}}\right)}{\left(\frac{\dot{V}_1}{V_{1,m}} + \frac{\dot{V}_2}{V_{2,m}}\right)^2} \tag{4.8}$$

$$\Delta\dot{V} = 0.5\% \cdot \dot{V} \tag{4.9}$$

$$\Delta\rho = 0.02\% \cdot \rho \tag{4.10}$$

$$V^{\text{E}} = \frac{x_1 M_1 + x_2 M_2}{\rho} - x_1 V_{1,m} - x_2 V_{2,m} \tag{4.11}$$

$$\Delta V^{\text{E}} = \frac{\rho(\Delta x_1 M_1 + \Delta x_2 M_2) - (x_1 M_1 + x_2 M_2)\Delta\rho}{\rho^2} - x_1 V_{1,m} - x_2 V_{2,m} \tag{4.12}$$

where $\dot{V}_i$ is the volumetric flow of the component i; $V_{i,m}$ is the molar volume of the component i; ρ is the density; and M_i is the molar mass

of component i. The percentage factors in the expressions for $\dot{V}$ and ρ in equations 4.9 and 4.10 originate from the calibration of the instruments. The uncertainty of the volumetric flow $\Delta\dot{V}$ was checked by analyzing the time averaged mass flow of well-known fluid by weighing the product on a balance. The value, 0.5 % in the equation 4.9 was the maximum deviation of the experimental value from the calculated volumetric flow. The uncertainty of the density $\Delta\rho$ was obtained through calibration with well-known reference components. The value of 0.02 % in the equation 4.10 was the deviation from the best straight line representing the experimental density.

5. Results

In this chapter, the results of the attached publications are first summarized in tables 5.1 and 5.2. Then, the main results of the measured thermodynamic properties (VLE, γ_i, H^E, V^E) of each category of studied binary systems are briefly highlighted.

Table 5.1. Summary of the Measured VLE Data.

Equip-ment	System	T / K	p / kPa	No. Points	Ref.
Static	Isobutane + MeOH	364.5	267.5–1686.4	27	I
Static	Isobutane + 2-PrOH	364.5	144.2–1686.3	27	I
Static	Isobutane + 2-BuOH	364.5	74.1–1686.3	27	I
Static	Isobutane + TBA	364.5	142.6–1685.6	27	I
Circ. still	MIBK + 2-BuOH	368	53.2–85.2	19	II
Circ. still	MIBK + *t*-PnOH	368	53.4–78.3	25	II
Circ. still	MIBK + 2-EH	388	8.8–98.7	20	II
Circ. still	TAEE + 1-BuOH	358	27.4–61.0	23	III
Circ. still	TAEE + 2-BuOH	358	57.3–61.3	30	III
Circ. still	TAEE + *t*-PnOH	358	52.8–61.0	26	III
Circ. still	EtOAc + 2-BuOH	350	41.0.–100.7	22	IV
Circ. still	2-BuOH + BuOAc	350	19.2–41.0	17	IV
Circ. still	EtOAc + BuOAc	350	19.2–100.7	24	IV
Circ. still	ETBE + ACN	333	49.8–64.3	23	V
Circ. still	TAEE + ACN	343	34.4–71.2	26	V
Circ. still	TAEE + PPN	363	70.1–80.7	32	V
HS-GC	MIBK + 2-BuOH	368		11	II
HS-GC	MIBK + *t*-PnOH	294.7		11	II
HS-GC	MIBK + *t*-PnOH	333.2		14	II
HS-GC	MIBK + *t*-PnOH	368.2		35	II

Table 5.2. Summary of the Measured H^E Data with SETARAM C80 Calorimeter and V^E Data with the DMA 512P Densimeter at 298 K and at 101.325 kPa.

Data Type	System	T / K	p / kPa	No. Points	Ref.
$H^E + V^E$	MIBK + 2-BuOH	298	101.32	10+10	II
$H^E + V^E$	MIBK + *t*-PnOH	298	101.32	10+10	II
$H^E + V^E$	MIBK + 2-EH	298	101.32	10+10	II
$H^E + V^E$	TAEE + 1-BuOH	298	101.32	9+9	III
$H^E + V^E$	TAEE + 2-BuOH	298	101.32	9+9	III
$H^E + V^E$	TAEE + *t*-PnOH	298	101.32	9+9	III
$H^E + V^E$	EtOAc + 2-BuOH	298	101.32	9+9	IV
$H^E + V^E$	2-BuOH + BuOAc	298	101.32	9+9	IV
$H^E + V^E$	EtOAc + BuOAc	298	101.32	9+9	IV
$H^E + V^E$	ETBE + ACN	298	101.32	9+9	V
$H^E + V^E$	ETBE + PPN	298	101.32	9+9	V
$H^E + V^E$	TAEE + ACN	298	101.32	9+9	V
$H^E + V^E$	TAEE + PPN	298	101.32	9+9	V

5.1 Results of the Binary Systems of an Alkane + Alcohols

The thermodynamic properties of binary mixtures containing isobutane and methanol (MeOH), 2-propanol (2-PrOH), 2-butanol (2-BuOH), and *tert*-butanol (TBA) were studied in publication I. The vapor–liquid equilibrium of the measured binary systems are shown in figure 5.1 and the calculated activity coefficients in figure 5.2. As seen in the figure, the system behaves more ideally the longer the chain length and the higher the branching of the alcohol is.

The data showed good quality as the experimental points coincided when approaching the equimolar composition from both ends. The consistency tests were not performed, since the data consistency requirements were satisfied in the data reduction. As seen in figure 5.1, azeotropic behavior was observed at T = 364.5 K only for the binary system of isobutane (1) + methanol (2) at x = 0.871 and p = 1822 kPa.

5.2 Results of the Binary Systems of a Ketone + Alcohols

The thermodynamic properties of the binary mixtures containing methyl isobutyl ketone (MIBK) and 2-butanol (2-BuOH), *tert*-pentanol (*t*-PnOH),

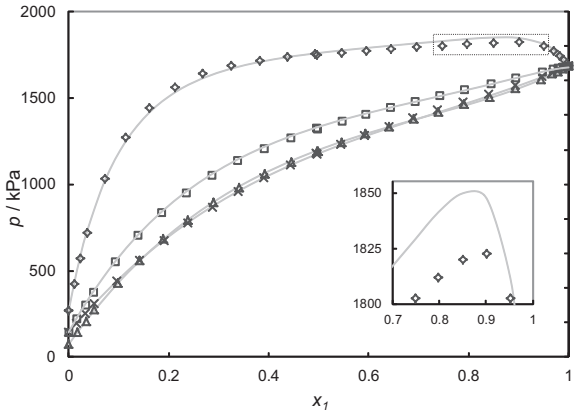

Figure 5.1. Pressure p and isobutane liquid mole fraction x_1 diagram for isobutane (1) ◇, + methanol; □, + 2-propanol; △, + 2-butanol; × + TBA; —, comparison with Legendre polynomial regressions. The azeotropic point of the binary system of isobutane + methanol is shown enlarged.

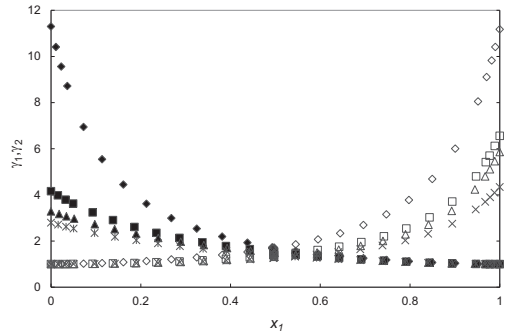

Figure 5.2. Activity coefficients: ◇, isobutane (1) + ♦, methanol (2); □, isobutane (1) + ■, 2-propanol (2); △, isobutane (1) + ▲, 2-butanol (2); ×, isobutane (1) + ∗, TBA (2); —, comparison with Legendre polynomial regressions. The azeotropic point of the binary system of isobutane + methanol is shown enlarged.

and 2-ethyl-1-hexanol (2-EH) were studied in publication II. The isothermal VLE data for the binary systems of MIBK + 2-BuOH and MIBK + *t*-PnOH were first measured at 368 K and for the binary system of MIBK + 2-EH at 388 K by using the circulation still. In addition for the binary system of MIBK + *t*-PnOH, isothermal data was measured at three temperatures: 294.7 K, 333.2 K, and 368.2 K by using HS-GC.

In the HS-GC data processing, the liquid phase sample concentrations

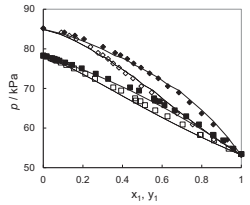

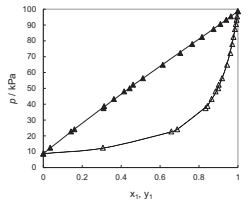

(a) VLE of MIBK + 2-BuOH
VLE of MIBK + *t*-PnOH

(b) VLE of MIBK + 2-EH

Figure 5.3. Pressure composition diagrams. (a) MIBK (1) + 2-BuOH (2) at 368 K: ⧫, liquid mole fraction; ◇, vapor mole fraction; MIBK (1) + *t*-PnOH (2) at 368 K: ■, liquid mole fraction, □, vapor mole fraction. (b) MIBK (1) + 2-EH (2) at 368 K: ▲, liquid mole fraction, △, vapor mole fraction. —, liquid phase model, · · ·, vapor phase model.

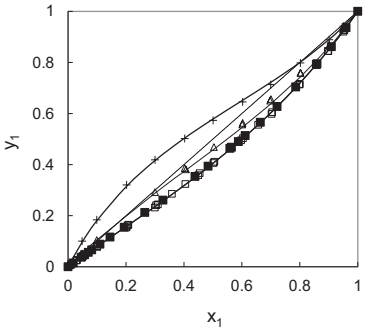

Figure 5.4. Composition diagram for MIBK (1) + *t*-PnOH (2): ■ circulation still at 368 K, □ HS-GC at 368 K, △ HS-GC at 333 K, + HS-GC at 294 K ; —, comparison with the model in publication II.

were corrected for the difference due to vapor phase sampling [45]. The ideal gas assumption was used for vapor phase and the UNIFAC (Dortmund) [22] activity coefficient model for the liquid phase.

All the VLE data obtained through measurements with the circulation still and the HS-GC were included in the VLE model together with the measured H^E data. Two types of VLE equipment enabled the use of a wider experimental data range in the model and also showed good fit together. Only the binary system of MIBK + *t*-PnOH showed an azeotropic behavior at 294 K at the composition $x = 0.7673$ (see figure 5.4).

The excess enthalpies were highly positive and close to each other for all

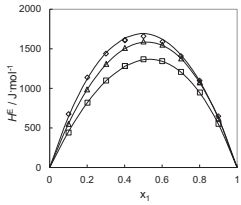

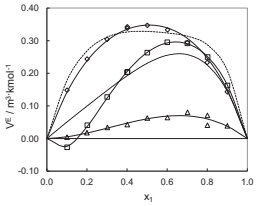

(a) Excess molar enthalpies H^E **(b)** Excess molar volumes V^E

Figure 5.5. Excess properties. (a) Excess molar enthalpies H^E at 298 K of binary systems of MIBK (1) + an alcohol (2) { ◇, + 2-butanol; □, + *tert*-pentanol; △, + 2-ethyl-1-hexanol }, —, comparison with the model. (b) Excess molar volumes V^E at 298 K of binary systems of MIBK (1) + an alcohol (2) { ◇, + 2-butanol; □, + *tert*-pentanol; △, + 2-ethyl-1-hexanol }, —, Redlich–Kister model; ···, literature [46]; - – -, literature [47].

three binary systems (see figure 5.5). The highest values were observed for the binary system of MIBK + 2-BuOH, and the lowest for the binary system of MIBK + *t*-PnOH.

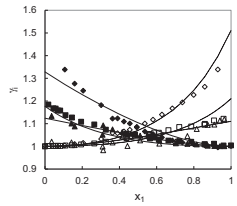

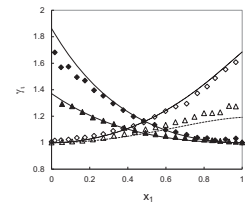

(a) Measured γ_i **(b)** Extrapolated γ_i

Figure 5.6. Activity coefficients for binary systems of MIBK (1) + an alcohol (2): (a) ♦, MIBK + ◇, 2-BuOH at 368 K; ■, MIBK + □, *t*-PnOH at 368 K; ▲, MIBK + △, 2-EH at 388 K; —, modeled MIBK activity coefficients, ···, modeled alcohol activity coefficients. (b) A comparison of activity coefficients obtained from literature [48] against modeled activity coefficients at 20 kPa and 101 kPa , ♦ (MIBK), ◇ (2-BuOH) measurements at 20 kPa; and ▲ (MIBK), △ (2-BuOH) measurements at 101 kPa; —, modeled MIBK activity coefficients, ···, modeled alcohol activity coefficients.

The thermodynamic model was extrapolated to isobaric measurements and compared with literature data [48]. The measured and modeled activity coefficients are presented in figure 5.6. As seen in the figure, the excess enthalpy gave good temperature dependency for the activity coefficients in extrapolation outside the original temperature range.

5.3 Results of the Binary Systems of an Ether + Alcohols

The measured and modeled thermodynamic data for the binary systems of TAEE + an alcohol (1-BuOH, 2-BuOH, or *t*-PnOH) are presented in detail in publication III. All three binary systems with TAEE showed azeotropic behavior that is seen in figure 5.7 and in table 5.3. The table lists the azeotropic compositions and pressures at 358 K for the binary systems. The azeotropic points at the studied temperatures were located in the middle part of the composition range for the binary systems of TAEE + 2-BuOH and TAEE + *t*-PnOH. For the binary system of TAEE + 1-BuOH the azeotropic composition was located in the dilute range of the alcohol.

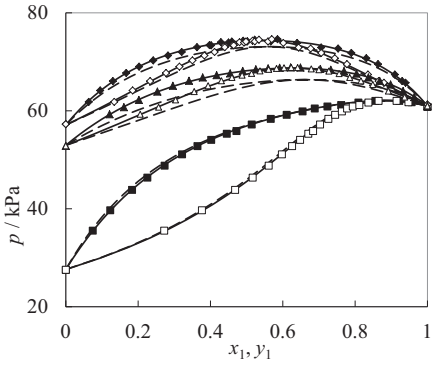

Figure 5.7. Experimental (vapor + liquid) equilibrium for pressure p, liquid molefraction x, and vapor mole fraction y at temperature $T = 358$ K. TAEE (1) + 1-BuOH (2): ■, liquid, □, vapor; TAEE (1) + 2-BuOH (2): ♦, liquid, ◇, vapor; TAEE (1) + *t*-PnOH (2): ▲, liquid, △, vapor; —, Wilson model; ···, UNIFAC (Dortmund) model.

The figure 5.7 shows that the Wilson activity coefficient model agreed better with the experiments in comparison to the UNIFAC (Dortmund) model [22]. This was presumable since the UNIFAC model [21] is a predictive model whereas the Wilson model is a model with adjustable parameters.

Table 5.3. Azeotropic Composition for the Systems TAEE (1) + an Alcohol (2) {1-Butanol, 2-Butanol, or *tert*-Pentanol} at 358 K.

Alcohol	x_1	p / kPa
1-BuOH	0.883	62.2
2-BuOH	0.546	74.6
t-PnOH	0.626	68.9

The figure 5.8 shows the excess properties. The excess enthalpies were positive but slightly lower than those of the binary systems of alcohols and the ketone. For the binary systems consisting of TAEE and a butanol, the H^E were almost the same whereas the increase by one in the carbon number of the alcohol lowered the maximum value by one third. Unlike the binary systems of the ketone and alcohols, the excess volumes were negative throughout the composition ranges. Interestingly, even though the values of H^E were of the same magnitude for all three binary systems, the V^E of the binary system of TAEE and *t*-PnOH differed remarkably from those of the binary systems consisting of TAEE and 1-BuOH or 2-BuOH.

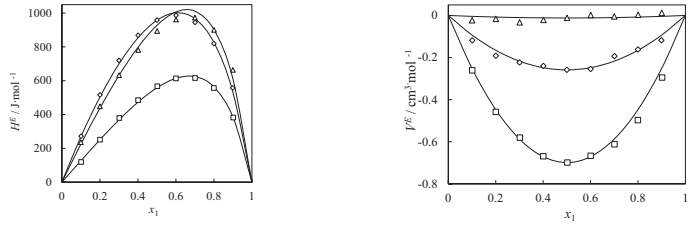

(a) Excess molar enthalpies H^E **(b)** Excess molar volumes V^E

Figure 5.8. Excess properties. (a) Excess molar enthalpies H^E at 298 K of binary systems of TAEE (1) + an alcohol (2) { □, + 1-BuOH; ◇, + 2-BuOH;△, + *t*-PnOH }, —, comparison with the Wilson model. (b) Excess molar volumes V^E at 298 K of binary systems of TAEE (1) + an alcohol (2) { □, + 1-BuOH; ◇, + 2-BuOH; △, + *t*-PnOH }, —, Redlich–Kister model

The figure 5.9 represents the measured and modeled activity coefficients. The activity coefficents moderately differ from unity: the upper limit for the values is three. Only the best-suited Wilson model is used for comparison with the experimental activity coefficients.

5.4 Results of the Binary Systems of Esters + Alcohol

The thermodynamic properties of the binary mixtures of two esters and one alcohol were studied in publication IV. The VLE was measured at 350 K and the excess properties at 298 K and at 101.325 kPa.

The selected components were ethyl acetate (EtOAc), butyl acetate (BuOAc), and 2-butanol (2-BuOH). The acetate-alcohol binary mixtures highly differed from an ideal mixture whereas the EtOAc-BuOAc mixture behaved nearly ideally.

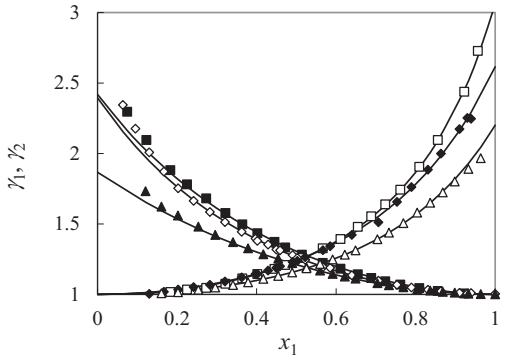

Figure 5.9. Activity coefficients at 358 K. TAEE (1) + 1-BuOH: □, TAEE, ■, 1-BuOH; TAEE (1) + 2-BuOH (2): ♦, TAEE, ◇, 2-BuOH; TAEE (1) + *t*-PnOH (2): △, TAEE, ▲, *t*-PnOH; —, Wilson model.

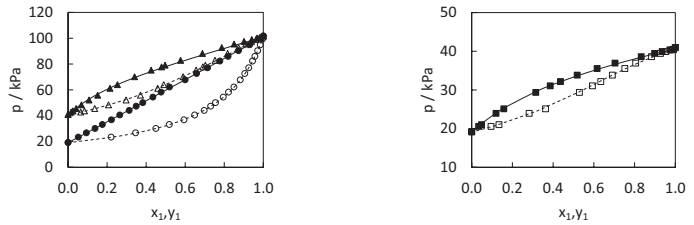

(a) VLE of EtOAc + 2-BuOH VLE of EtOAc + BuOAc

(b) VLE of 2-BuOH + BuOAc

Figure 5.10. Pressure composition diagrams at 350 K. (a) EtOAc (1) + 2-BuOH (2) : *blacktriangle*, liquid mole fraction; △, vapor mole fraction; EtOAc (1) + BuOAc (2) : •, liquid mole fraction, ○, vapor mole fraction. (b) 2-BuOH (1) + BuOAc (2): ■, liquid mole fraction, □, vapor mole fraction. —, liquid phase model, ···, vapor phase model.

The figure 5.10 illustrates the VLE of the measured systems. No azeotropes were observed at 350 K even though the compositions of vapor and liquid phase were very close to each other at high concentrations of the more volatile component.

The figure 5.11 shows the measured excess properties H^E and V^E in this work. No H^E data were available in open literature but the comparison with the available V^E data is presented in the figure.

Our results for the binary systems of an acetate + the alcohol are in line with the literature data [49, 50, 51]. For the nearly ideally behaving acetate–acetate binary mixture no V^E data were available in the open

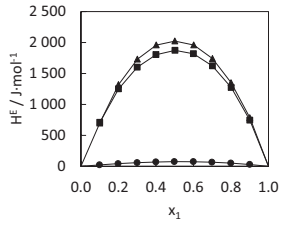

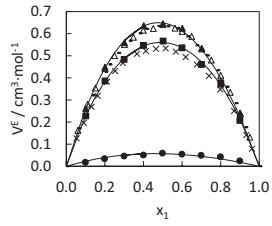

(a) Excess molar enthalpies H^E **(b)** Excess molar volumes V^E

Figure 5.11. Excess properties. (a) Excess molar enthalpies H^E at 298 K of binary systems of ▲, EtOAc (1) + 2-BuOH (2); ■, 2-BuOH (1) and BuOAc (2); ●, EtOAc (1) + BuOAc (2); —, Wilson model. (b) Excess molar volumes V^E at 298 K of binary systems of ▲, EtOAc (1) + 2-BuOH (2); ■, 2-BuOH (1) + BuOAc (2); ●, EtOAc (1) + BuOAc (2); —, Wilson model; –, EtOAc (1) + 2-BuOH (2) from literature [49]; △, EtOAc (1) + 2-BuOH (2) from literature [50]; ×, 2-BuOH (1) + BuOAc (2) from literature [51].

literature. A clear difference is seen between the highly nonideal acetate–alcohol binary mixtures and the practically ideal acetate-acetate binary mixture.

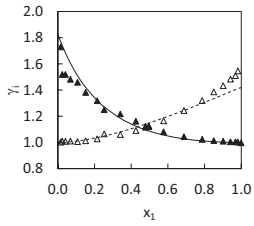

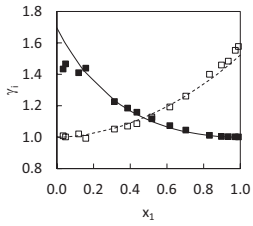

(a) γ_i of EtOAc + 2-BuOH **(b)** γ_i of 2-BuOH + BuOAc

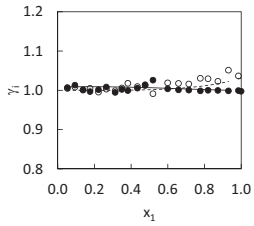

(c) γ_i of EtOAc + BuOAc

Figure 5.12. Activity coefficients: (a) ▲, EtOAc + △, 2-BuOH at 350 K. (b) ■, 2-BuOH, □, BuOAc at 350 K. (c) ●, EtOAc, ○, BuOAc at 350 K. —, modeled activity coefficients of component (1), · · ·, modeled activity coefficients of the component (2).

The figures of the activity coefficients 5.12a - 5.12b confirm the same division between closely ideally and nonideally behaving mixtures: the activity coefficients show higher deviation from unity for the acetate–alcohol mixtures whereas for the acetate–acetate mixture the activity coefficients are practically one.

5.5 Results of the Binary Systems of Ethers + Nitriles

The thermodynamic properties of the binary systems of two ethers, ETBE and TAEE, and two nitriles, acetonitrile (ACN) and propanenitrile (PPN), were studied in publication V.

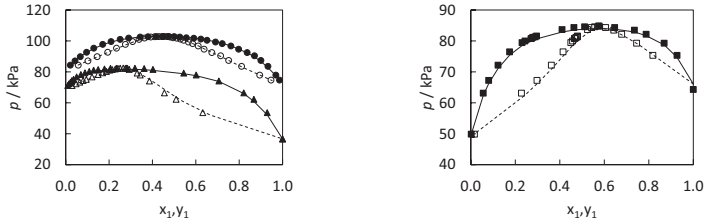

(a) VLE of ETBE + ACN at 333 K
VLE of TAEE + ACN at 343 K

(b) VLE of TAEE + PPN at 363 K

Figure 5.13. Pressure composition diagrams. (a) ETBE (1) + ACN (2) at 333 K: ■, liquid mole fraction; □, vapor mole fraction. (b) TAEE (1) + ACN (2) at 343 K: ▲, liquid mole fraction, △, vapor mole fraction; TAEE (1) + PPN (2) at 363 K: ●, liquid mole fraction, ○, vapor mole fraction. —, liquid phase model, ···, vapor phase model.

The isothermal VLE data was measured at 333 K for the binary system of ETBE + ACN, at 343 K for the binary system of TAEE + ACN, and at 363 K for the binary system of TAEE + PPN. The experimental VLE data with the model predictions of the studied binary systems of ethers and nitriles are shown in figures 5.13a and 5.13b. The VLE of the binary system of ETBE and PPN was not measured since this data were already available in literature [52].

As seen in the figures and in table 5.4, all studied mixtures exhibit maximum-pressure azeotropes that were located at the mid-range composition. A comparison between the experiments and the model reveals that the model successfully predicted the azeotropic compositions.

The excess enthalpies of the measured binary systems were clearly positive as shown in figure 5.14a. The mixtures containing ACN gave higher

Table 5.4. Experimental and Modeled Azeotropic Molar Fractions x for the Binary Systems of ETBE, ACN, and PPN at Temperature T.

		Experiments	Model
	T / K	x_1	x_1
ETBE (1) - ACN (2)	333	0.5927	0.5908
TAEE (1) - ACN (2)	343	0.2559	0.2674
TAEE (1) - PPN (2)	363	0.4402	0.4459

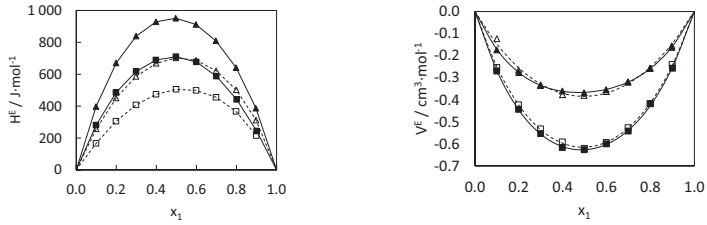

(a) Excess molar enthalpies H^E **(b)** Excess molar volumes V^E

Figure 5.14. Excess properties at 298 K. ETBE (1) + ACN (2): ■; TAEE (1) + ACN (2): ▲; ETBE (1) + PPN (2): □; TAEE (1) + PPN (2): △. —, model for the binary systems containing ACN, · · ·, model for the binary systems containing PPN.

values in comparison to the mixtures containing PPN.

In the case of V^E, the choice of the ether had more effect on the magnitude of the excess property than the choice of the nitrile (see figure 5.14b). For both excess properties, the mixtures containing PPN had lower absolute values than the mixtures containing ACN.

The activity coefficients of the binary systems of nitriles and ethers are shown in figures 5.15a – 5.15c. The model indicated the highest infinite dilution activity coefficients for the binary mixture of TAEE and ACN. The activity coefficients of the binary mixture of TAEE and ACN were only slightly lower. Contrary to ACN containing mixtures, the values of the activity coefficients for the binary mixture of ETBE and PPN were approximately half of the corresponding values of the binary mixture of ETBE + ACN.

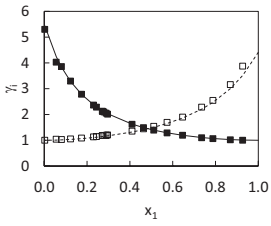

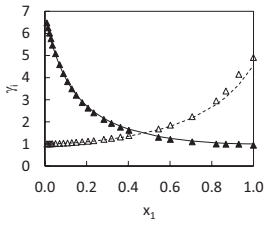

(a) γ_i for ETBE (1) + ACN (2) at 333 K **(b)** γ_i for TAEE (1) + ACN (2) at 343 K

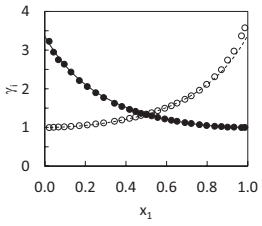

(c) γ_i for TAEE (1) + PPN (2) at 363 K

Figure 5.15. Activity coefficients: (a) ■, ETBE; □, ACN. (b) ▲, TAEE, △, ACN. (c) •, TAEE, ○, PPN. —, modeled activity coefficients of the ether, ···, modeled activity coefficients of the nitrile.

6. Conclusions

The aim of this thesis was to study the following thermodynamic properties, vapor–liquid equilibrium (VLE), excess enthalpy (H^{E}), and excess volume (V^{E}) both experimentally and by modeling. The pure components and their binary mixtures were selected to benefit process industry and the emphasis of the modeling was in phase behavior. The goals were achieved by providing new data and new parameters for thermodynamic models for five different categories of binary mixtures: alkanes, ethers, ketones, or esters with alcohols; and ethers with nitriles.

The focus was on two groups of components, of which the first one consisted of components that can be present in bio-based feedstocks. These components were alcohols, ethyl acetate, and butyl acetate. In the second group, the components that were considered as substitutes for oil-based components were studied. These comprised ETBE, TAEE, EtOAc, and BuOAc. In addition, the components inherent in the component manufacturing processes were included in this study. The thermodynamic data on mixtures of the components of these components were scarcely studied so this work provided alleviation for the problem by filling the data gaps.

Five different experimental set-ups were used for acquiring new data. For VLE data, a static total pressure apparatus, a circulation still, and a headspace–gas chromatograph were utilized. For H^{E} data, a SETARAM C80 calorimeter with a flow mixing cell was succesfully implemented and applied to the experiments on selected binary systems. For V^{E} data, a vibrating tube density measuring cell was used. In the measurements of the H^{E}, the power of the simultaneous use of the densimeter was found to support the objective to produce high quality H^{E} data.

The studied systems were modeled with the Wilson activity coefficient model that in comparison with NRTL, UNIFAC, and UNIQUAC models showed better accuracy in the case of the binary systems of TAEE and

alcohols. Two models for fugacity coefficients were used: Soave–Redlich–Kwong equation of state and Hayden-O'Connell method with the chemical theory. The selected methods succeeded in modeling the nonideality of the vapor phase. For nearly ideally behaving mixture, the ideal liquid assumption together with the ideal vapor assumption sufficiently predicted the VLE. The excess properties, however, can not be traced by using ideality assumption. The excess properties enabled the model for extrapolation beyond the experimental temperature and pressure range which was also confirmed by a case study.

Bibliography

[1] Aittamaa, J. and Pokki, J.-P. (2004) *VLEFIT A Program package to obtain parameters in models of activity coefficient from VLE data (Manual)*. Espoo.

[2] Laavi, H. (2010) *Phase behavior in chemical reactor*. Licentiate's thesis, Aalto University, Espoo.

[3] Alopaeus, V., Laavi, H., and Aittamaa, J. (2008) A dynamic model for plug flow reactor state profiles. *Comput. Chem. Eng.*, **32**, 1494–1506.

[4] Laavi, H., Qu, Q., Lipiäinen, K., and Alopaeus, V. (2009) Applying kinetics over phase boundaries. *8th World Congress of Chemical Engineering (WCCE8), Montreal, Quebec, Canada, August 23–27*.

[5] Carlson, E. (1996) Don't gamble with physical properties for simulations. *Chem. Eng. Prog.*, **92**, 35–46.

[6] European Fuel Oxygenates Association (EFOA). (accessed January 14, 2013) http://www.efoa.eu/en/fuel-ethers/what-are-fuel-ethers/how-are-fuel-ethers-made.aspx.

[7] Sundberg, A., Uusi-Kyyny, P., Jakobsson, K., and Alopaeus, V. (2012) A small scale pilot plant demonstration – case study of the synthetisation of 2-ethoxy-2-methylbutane. *AIChE Spring Meeting*, Houston, Texas, April 1–5, p. 7.

[8] Ruiz, D. A. (July 16, 2009), Fuel additive *U.S. Patent Application* 20090178331.

[9] Burgazli, J., Burton, J., and Daniels, D. (January 14, 2010), Fuel composition with enhanced low temperature properties *U.S. Patent Application* 20100005706.

[10] Ali, S. H., Al-Rashed, O., Azeez, F. A., and Merchant, S. Q. (2011) Potential biofuel additive from renewable sources – Kinetic study of formation of butyl acetate by heterogeneously catalyzed transesterification of ethyl acetate with butanol. *Bioresour. Technol.*, **102**, 10094–10103.

[11] European Fuel Oxygenates Association (EFOA). (accessed March 21, 2013) http://www.efoa.eu/en/markets.aspx.

[12] Walas, S. M. (1985) *Phase equilibria in chemical engineering*. Boston, MA: Butterworths.

[13] Redlich, O. and Kwong, J. N. S. (1949) On the thermodynamics of solutions. V. An equation of state. Fugacities of gaseous solutions. *Chem. Rev.*, **44**, 233–244.

[14] Soave, G. (1972) Equilibrium constants from a modified Redlich-Kwong equation of state. *Chem. Eng. Sci.*, **27**, 1197–1203.

[15] Sandler, S. I. (1999) *Chemical and engineering thermodynamics*. John Wiley & Sons, Inc., 3rd edn.

[16] Barker, J. (1953) Determination of activity coefficients from total pressure measurements. *Aust. J. Chem.*, **6**, 207–210.

[17] Hayden, J. G. and O'Connell, J. P. (1975) A generalized method for predicting second virial coefficients. *Ind. Eng. Chem. Proc. Des. Dev.*, **14**, 209–216.

[18] Prausnitz, J. M., Anderson, T. F., Grens, E. A., Eckert, C. A., Hsieh, R., and O'Connell, J. P. (1980) *Computer calculations for multicomponent vapour–liquid and liquid–liquid equilibria*. Prentice Hall.

[19] Wilson, G. M. (1964) Vapor–liquid equilibrium. XI. A new expression for the excess free energy of mixing. *J. Am. Chem. Soc.*, **86**, 127–130.

[20] Renon, H. and Prausnitz, J. M. (1968) Local compositions in thermodynamic excess functions for liquid mixtures. *AIChE J.*, **14**, 135–144.

[21] Abrams, D. S. and Prausnitz, J. M. (1975) Statistical thermodynamics of liquid mixtures: A new expression for the excess Gibbs energy of partly or completely miscible systems. *AIChE J.*, **21**, 116–128.

[22] Weidlich, U. and Gmehling, J. (1987) A modified UNIFAC model. 1. Prediction of VLE, hE, and γ^{infty}. *Ind. Eng. Chem. Res.*, **26**, 1372–1381.

[23] Gmehling, J. and Onken, U. (1977) Vapor–liquid equilibrium data collection. Aquaeous-organic systems. *DECHEMA Data Series, Vol. 1 Part 1*, DECHEMA Frankfurt/Main.

[24] Rackett, H. (1970) Equation of state for saturated liquids. *J. Chem. Eng. Data*, **15**, 514–517.

[25] Pokki, J.-P. (2004) *Development of vapour liquid equilibrium calculation methods for chemical engineering design*. Ph.D. thesis, Helsinki University of Technology.

[26] Atkins, P. W. (1998) *Physical Chemistry*. Oxford University Press, 6 edn.

[27] Kojima, K., Moon, H. M., and Ochi, K. (1990) Thermodynamic consistency test of vapor-liquid equilibrium data: – Methanol ∼ water, benzene ∼ cyclohexane and ethyl methyl ketone ∼ water –. *Fluid Phase Equilib.*, **56**, 269–284.

[28] Kurihara, K., Egawa, Y., Ochi, K., and Kojima, K. (2004) Evaluation of thermodynamic consistency of isobaric and isothermal binary vapor–liquid equilibrium data using the PAI test. *Fluid Phase Equilib.*, **219**, 75–85.

[29] Kurihara, K., Egawa, Y., Iino, S., Ochi, K., and Kojima, K. (2007) Evaluation of thermodynamic consistency of isobaric and isothermal binary vapor–liquid equilibrium data using the PAI test II, alcohol + n-alkane, +aromatic, +cycloalkane systems. *Fluid Phase Equilib.*, **257**, 151–162.

[30] Luis, P., Wouters, C., Sweygers, N., Creemers, C., and Bruggen, B. V. D. (2012) The potential of head-space gas chromatography for VLE measurements. *J. Chem. Thermodyn.*, **49**, 128–136.

[31] Kolb, B. and Ettre, L. S. (1997) *Static Headspace–Gas Chromatography: Theory and Practice*. Wiley-VCH.

[32] Uusi-Kyyny, P., Pokki, J.-P., Laakkonen, M., Aittamaa, J., and Liukkonen, S. (2002) Vapor liquid equilibrium for the binary systems 2-methylpentane + 2-butanol at 329.2 K and *n*-hexane + 2-butanol at 329.2 and 363.2 K with a static apparatus. *Fluid Phase Equilib.*, **201**, 343–358.

[33] Hynynen, K., Uusi-Kyyny, P., Pokki, J.-P., Pakkanen, M., and Aittamaa, J. (2006) Isothermal vapor liquid equilibrium for 2-methylpropene + methanol, + 1-propanol, + 2-propanol, + 2-butanol, and + 2-methyl-2-propanol binary systems at 364.5 K. *J. Chem. Eng. Data*, **51**, 562–568.

[34] Ouni, T., Zaytseva, A., Uusi-Kyyny, P., Pokki, J.-P., and Aittamaa, J. (2005) Vapour–liquid equilibrium for the 2-methylpropane + methanol, +ethanol, +2-propanol, +2-butanol and +2-methyl-2-propanol systems at 313.15 K. *Fluid Phase Equilib.*, **232**, 90–99.

[35] Yerazunis, S., Plowright, J. D., and Smola, F. M. (1964) Vapor–liquid equilibrium determination by a new apparatus. *AIChE J.*, **10**, 660–665.

[36] Uusi-Kyyny, P., Pokki, J. P., Aittamaa, J., and Liukkonen, S. (2001) Vapour–liquid equilibrium for the binary systems of methanol + 2,4,4-trimethyl-1-pentene at 331 K and 101 kPa and methanol + 2-methoxy-2,4,4-trimethylpentane at 333 K. *J. Chem. Eng. Data*, **46**, 1244–1248.

[37] Sapei, E., Zaytseva, A., Uusi-Kyyny, P., Keskinen, K. I., and Aittamaa, J. (2007) Vapor–liquid equilibrium for binary system of thiophene + 2,2,4-trimethylpentane at 343.15 and 353.15 K and thiophene + 2-ethoxy-2-methylpropane at 333.15 and 343.15 K. *Fluid Phase Equilib.*, **261**, 115–121.

[38] SETARAM (2010) *Technical note 12 – C80 Flow mixing cell*. Caluire, France.

[39] Wadsö, I. and Goldberg, R. (2001) Standards in isothermal microcalorimetry: (IUPAC Technical Report). *Pure Appl. Chem.*, **73**, 1625–1639.

[40] Poledníček, M. (2000) *Development of instruments for obtaining thermodynamic data in systems of environmental and energetic interest*. Ph.D. thesis, Blaise Pascal University, Clermont-Ferrand, France.

[41] Wagner, W. and Pruß, A. (2002) The IAPWS formulation 1995 for the thermodynamic properties of ordinary water substance for general and scientific use. *J. Phys. Chem. Ref. Data*, **31**, 387–535.

[42] Lemmon, E. W., Jacobsen, R. T., Penoncello, S. G., and Friend, D. G. (2000) Thermodynamic properties of air and mixtures of nitrogen, argon, and oxygen from 60 to 2000 K at pressures to 2000 MPa. *J. Phys. Chem. Ref. Data*, **29**, 331–385.

[43] Laakkonen, M., Pokki, J.-P., Uusi-Kyyny, P., and Aittamaa, J. (2003) Vapour–liquid equilibrium for the 1-butene + methanol, + ethanol, + 2-propanol, + 2-butanol and + 2-methyl-2-propanol systems at 326 K. *Fluid Phase Equilib.*, **206**, 237–252.

[44] Raal, J. D. and Mühlbauer, A. L. (1998) *Phase Equilibria, Measurement and Computation*. Taylor & Francis.

[45] Westerholt, A., Liebert, V., and Gmehling, J. (2009) Influence of ionic liquids on the separation factor of three standard separation problems. *Fluid Phase Equilib.*, **280**, 56–60.

[46] Riggio, R., Ramos, J. F., Ubeda, M. H., and Espindola, J. A. (1981) Mixtures of methyl isobutyl ketone with three butanols at various temperatures. *Can. J. Chem.*, **59**, 3305–3308.

[47] Sólimo, H. N., Riggio, R., and Martinez, H. E. (1986) Excess thermodynamic properties for methyl isobutyl ketone + tert-amyl alcohol system at 25°C. *J. Solution Chem.*, **15**, 283–289.

[48] Martínez, N. F., Lladosa, E., Burguet, M., Montón, J. B., and Yazimon, M. (2009) Isobaric vapour–liquid equilibria for the binary systems 4-methyl-2-pentanone + 1-butanol and + 2-butanol at 20 and 101.3 kPa. *Fluid Phase Equilib.*, **277**, 49–54.

[49] Hernández, P. and Ortega, J. (1997) Vapor–liquid equilibria and densities for ethyl esters (ethanoate to butanoate) and alkan-2-ol (C_3–C_4) at 101.32 kPa. *J. Chem. Eng. Data*, **42 (6)**, 1090–1100.

[50] Resa, J. M., González, C., Juez, M., and Ortiz de Landaluce, S. (2004) Density, refractive index and speed of sound for mixtures of ethyl acetate with 2-butanol and 3-methyl-1-butanol: Vapor–liquid equilibrium of the ethyl acetate + 3-methyl-1-butanol system. *Fluid Phase Equilib.*, **217**, 175–180.

[51] González, E. and Ortega, J. (1996) Vapor–liquid equilibria at 101.32 kPa in mixtures formed by the first four butyl alkanoates and butan-2-ol. *Fluid Phase Equilib.*, **124**, 161–175.

[52] Haimi, P., Uusi-Kyyny, P., Pokki, J.-P., and Alopaeus, V. (2010) Phase equilibrium measurements for systems containing propanenitrile with *tert*-butyl ethyl ether and C4-hydrocarbons. *Fluid Phase Equilib.*, **299**, 148–160.

To meet the increasing needs of process modeling, accurate thermodynamic data are needed for proper estimation of the phenomena taking place in chemical processes. The aim of this work was to provide accurate vapor–liquid equilibrium (VLE) data and models for industrially relevant systems. To make the thermodynamic model workable beyond the experimental temperature range, excess enthalpy data were provided. In this work, the studied chemicals were examples of typical groups of chemicals used in chemical industry or potential options to meet the increasing interest on bio-refinery related components. The studied systems were alcohols with alkanes, ethers, ketones, or esters. In addition, examples of binary systems of ethers with nitriles were included.

Aalto-DD 121/2013

ISBN 978-952-60-5271-7
ISBN 978-952-60-5272-4 (pdf)
ISSN-L 1799-4934
ISSN 1799-4934
ISSN 1799-4942 (pdf)

Aalto University
School of Chemical Technology
Department of Biotechnology and Chemical Technology
www.aalto.fi